



**US Army Corps
of Engineers®**
Engineer Research and
Development Center

ERDC
INNOVATIVE SOLUTIONS
for a safer, better world

Investigation of the Corrosion Mechanism and Determination of the EMS Estimated Service Life at Site 81

Vincent F. Hock Jr., Charles A. Weiss, Jr., Robert D. Moser,
Sean W. Morefield, and James B. Bushman

February 2013



The US Army Engineer Research and Development Center (ERDC) solves the nation's toughest engineering and environmental challenges. ERDC develops innovative solutions in civil and military engineering, geospatial sciences, water resources, and environmental sciences for the Army, the Department of Defense, civilian agencies, and our nation's public good. Find out more at www.erdcenter.usace.army.mil.

To search for other technical reports published by ERDC, visit the ERDC online library at <http://acwc.sdp.sirsi.net/client/default>.

Investigation of the Corrosion Mechanism and Determination of the EMS Estimated Service Life at Site 81

Vincent F. Hock Jr. and Sean W. Morefield

*US Army Engineer Research and Development Center (ERDC)
Construction Engineering Research Laboratory (CERL)
2902 Newmark Drive
PO Box 9005
Champaign, IL 61826-9005*

Charles A. Weiss Jr. and Robert D. Moser

*US Army Engineer Research and Development Center (ERDC)
Geotechnical and Structures Laboratory (GSL)
3909 Halls Ferry Road
Vicksburg, MS 39180*

James B. Bushman

*Bushman & Associates, Inc.
6395 Kennard Road
PO Box 425
Medina, OH 44256*

Final report

Approved for public release; distribution is unlimited.

Prepared for U.S. Army Corps of Engineers
Europe District
CMR 410, Box 1, APO, AE 09049

Under "Investigation of Corrosion Mechanism and Recommendations for Corrosion Mitigation."

Abstract

Structural damage resulting from corrosion of steel-clad structures can be of concern, especially when the steel is part of electromagnetic shielding of an underground structure. The US Army Corps of Engineers was called to lend assistance by having its corrosion experts and research laboratories investigate the condition and extent of corrosion at such a structure (Site 81) in Israel. This report documents the investigation, conclusions, and recommendations. In summary, from investigation and analyses of core samples, no significant corrosion was discovered and the estimated minimum service life of the existing structure is 199 years.

Contents

Abstract	ii
List of Figures and Tables.....	iv
Preface	vi
Unit Conversion Factors	viii
1 Introduction.....	1
1.1 Background.....	1
1.2 Objectives	1
1.3 Approach	2
1.3.1 Task 1.....	2
1.3.2 Task 2	2
1.3.3 Task 3.....	3
1.3.4 Task 4.....	3
2 Field Testing the Experimental Plan	4
3 Field Testing: August 9–17, 2012	8
4 Core Sample Testing	13
4.1 Methods.....	14
4.1.1 Acid-soluble chloride content analysis.....	14
4.1.2 Petrographic analysis	14
4.2 Results and discussion	15
4.2.1 Acid-soluble chloride content.....	15
4.2.2 Petrographic analysis.....	17
4.3 Conclusions of concrete core testing.....	34
5 Summary of Results	35
6 Recommendations.....	37
7 References	38
Appendix A: Water Testing.....	39
Appendix B: EMF Liner Corrosion Rate Measurement	42
Appendix C: As-Received Core Samples	45
Appendix D: Supplemental Photomicrographs.....	54
Report Documentation Page	

Figures and Tables

Figures

Figure 1. Step 1 of the in-situ LPR corrosion rate measurements.	4
Figure 2. Step 2 of the in-situ LPR corrosion rate measurements.	4
Figure 3. Step 3 of the in-situ LPR corrosion rate measurements.	5
Figure 4. Step 4 of the in-situ LPR corrosion rate measurements.	5
Figure 5. Step 5 of the in-situ LPR corrosion rate measurements.	6
Figure 6. Step 6 of the in-situ LPR corrosion rate measurements.	7
Figure 7. Step 7 of the in-situ LPR corrosion rate measurements.....	7
Figure 8. Existing trough in concrete liner over EMS steel plate.....	8
Figure 9. 16 in. diameter core hole cut to expose steel EMS for testing.....	8
Figure 10. Synthetic canvas bag containing two large instrument cases for transport to basement test site.	10
Figure 11. Epoxy injection overview.....	11
Figure 12. Two-part epoxy-mixing caulking gun.	11
Figure 13. Close-up photo of epoxy injection.	11
Figure 14. Close-up photo of holes after final placement of bolts.	11
Figure 15. Segments of reinforcing steel extracted at 2-3 in. depth from core sample #4 (left) and core sample #5 (right) with both showing minor surface corrosion.....	15
Figure 16. Photomicrographs of core sample #1 (5x above; 15x below).	18
Figure 17. Photomicrographs of core sample #3 (5x above; 15x below).	19
Figure 18. Photomicrographs of core sample #4 (5x above, 15x below).....	20
Figure 19. Photomicrographs of core sample #5 (5x above, 15x below).....	21
Figure 20. Photomicrographs of core sample #6 (5x above, 15x below).....	22
Figure 21. Photomicrographs of core sample #7 (5x above, 15x below).....	23
Figure 22. Photomicrographs of core sample #8 (5x above, 15x below).....	24
Figure 23. Photomicrographs of core sample #9 (5x above, 15x below).....	25
Figure 24. Photomicrographs of core sample #10 (5x above, 15x below).	26
Figure 25. Photomicrographs of core sample #11 (5x above, 15x below).	27
Figure 26. Photomicrographs of core sample #12 (5x above, 15x below).	28
Figure 27. Photomicrographs of core sample #13 (5x above, 15x below).....	29
Figure 28. Photomicrographs of core sample #14 (5x above, 15x below).	30
Figure 29. Photomicrographs of core sample #15 (5x above, 15x below).	31
Figure 30. Photomicrographs of core sample #16 (5x above, 15x below).	32
Figure 31. Photomicrographs of core sample #17 (5x above, 15x below).....	33

Tables

Table 1. Chloride content results from core samples #1-#11.....16
Table 2. Chloride content results from core samples #12-#17.....17

Preface

This study was conducted for the US Army Corps of Engineers, Europe District under the Project, “Investigation of Corrosion Mechanism and Recommendations for Corrosion Mitigation,” which was funded by Military Interdepartmental Purchase Request (MIPR) #W2SD0622151436. The technical monitor was Adam Beris of the U.S Army Corps of Engineers, Israel Area Office, Northern Israel Resident Office (CENAU-EC-CI-N).

The work was performed by the Structures and Materials Branch (CF-M) of the Facilities Division (CF), U.S. Army Engineer Research and Development Center – Construction Engineering Research Laboratory (ERDC-CERL) at Champaign, IL. At the time of publication, Ms. Vicki Van Blaricum was Chief, CEERD-CF-M; Mr. L. Michael Golish was Chief, CEERD-CF; and Mr. Marty Savoie was the Technical Director for Environmental Quality and Infrastructure. The Deputy Director of ERDC-CERL was Dr. Kirankumar V. Topudurti and the Director was Dr. Ilker R. Adiguzel.

Laboratory analysis was performed by the Concrete and Materials Branch (CMB), Engineering Systems and Materials Division (ESMD), U.S. Army Engineer Research and Development Center – Geotechnical and Structures Laboratory (ERDC-GSL) at Vicksburg, MS. At the time of publication, Christopher M. Moore was Chief, CMB; Dr. Larry N. Lynch was Chief, ESMD. The Deputy Director of ERDC-GSL was Dr. William P. Grogan and the Director was Dr. David W. Pittman.

COL Kevin J. Wilson was the Commander of ERDC, and Dr. Jeffery P. Holland was the Director.

Acknowledgements

The ERDC project delivery team (PDT) consisted of Mr. Vincent F. Hock, Mr. Sean W. Morefield, and Ms. Heather E. Johnson, ERDC-CERL; Dr. Robert D. Moser and Dr. Charles A. Weiss Jr., ERDC-GSL; and James B. Bushman, corrosion consultant. Laboratory assistance was provided by Mr. Kevin Torres-Cancel and Ms. Linda J. Ragan of the Concrete and Materials Branch (CMB) at ERDC-GSL. Additional analytical chemistry sup-

port was provided by the Environmental Chemistry Branch, Environmental Processes and Engineering Division of the ERDC Environmental Laboratory (ERDC-EL) in Vicksburg, MS.

Unit Conversion Factors

Multiply	By	To Obtain
cubic yards	0.7645549	cubic meters
feet	0.3048	meters
foot-pounds force	1.355818	joules
inches	0.0254	meters
microns	1.0 E-06	meters
pounds (force) per square inch	6.894757	kilopascals
pounds (mass)	0.45359237	kilograms

1 Introduction

1.1 Background

As part of an ongoing project and to add improvements to an existing underground structure, the structure's upper concrete overlay and galvanized steel plate comprising the electromagnetic shielding (EMS) were removed at selected locations. The galvanized steel plate was also removed at some wall locations. Almost all of the extracted plates exhibited some level of corrosion on the side that was in contact with the floor/wall concrete element while little or no corrosion was observed on the surface in contact with the 15–17 cm thick concrete overlay. Four samples were sent by the contractor to a laboratory which determined that the thickness of the corrosion was on the order of 100 microns.

Subsequently, several other locations were exposed and the visual results regarding corrosion found to be consistent with the initial findings. Although the total area of extracted galvanized steel plate is very small with respect to the total area of EMS, it is reasonable to assume that the corrosion problem is very likely present throughout the whole envelope. It is worthwhile noting that at some locations of the floor slab, the presence of water was observed in the interstitial space between the slab and the plate. The source of this water has not been categorically determined and is controversial; possible sources of the water include byproduct of saw cutting operations performed by the current contractor, leftover rain water accumulated during the original construction, mix-water remaining after cement hydration during concrete pour, and infiltration from the local groundwater due to possible damage in the waterproofing membrane. The extent of the water permeation is unknown at this time.

1.2 Objectives

The US Army Corps of Engineers was called to investigate the condition of and extent of corrosion on electromagnetic shielding at Site 81 in Israel. It was desired to estimate the remaining service life of the EMS based on observed conditions and measurements, and remediation courses if required.

1.3 Approach

A field investigation was performed by the corrosion expert from ERDC-CERL and the corrosion consultant to observe and document the existing site conditions as it related to corrosion of the EMS, to gather pertinent information, and to supervise the physical drilling and coring (Steps 1–7; see Chapter 2) of the concrete overlay, EMS steel plate, and underlying concrete slab. Sample removal and other required physical labor was performed by additional on-site personnel. In-situ testing to collect the necessary data was performed by the corrosion expert and consultant. After the field testing was completed, laboratory testing and engineering analysis occurred. The investigation included the four tasks given below.

1.3.1 Task 1

Review available information on existing conditions and issues, and develop a field and laboratory testing plan.

1.3.2 Task 2

Calibrate testing equipment, including all components required to perform on-site testing, and prepare for overseas shipping. Equipment to be provided includes the following instruments to perform in-situ linear polarization resistance (LPR) tests:

- 1 each — Gamry Reference 600™ Potentiostat DC/ AC corrosion measurement system
- 2 each — Computers with custom Gamry corrosion-rate software to operate potentiostat and analysis software to compile and summarize data.
- 2 each — Custom-built, project-specific counter electrodes of precious metal oxide-(PMO) coated titanium
- 2 each — Custom-built, project-specific reference electrodes of PMO-coated titanium
- Instruments to be used to perform measurement of the EMS steel plate corrosion potential at the concrete slab/steel interface:
- 1 each — Fluke® Meter Model 293, a 5-½ digit precision volt-ohm meter (VOM)
- 1 each — Fluke Meter Model 865, a VOM meter with oscilloscope function
- 1 Each — Extech® Model 381295, a dual-channel true RMS 5 MHz digital oscilloscope

- 1 Each — Extech Model 540, a 5-½ digit precision VOM recording meter
- 2 Each — Silver/silver chloride (Ag/AgCl) reference electrodes
- 1 Each — Digital camera with macro lens capability to focus 1 in. from lens.
- Multiple test lead wires as needed for project

1.3.3 Task 3

Perform a field investigation of existing conditions as it relates to the corrosion of existing steel plates at the project site in Tel Aviv, Israel. The field testing included the following steps.

1. In-situ LPR testing to determine the active corrosion rate of the steel EMS surface in contact with the concrete slab.
2. Measuring the EMS steel plate corrosion potential at the concrete slab/steel interface at each of the selected LPR test locations after coring through the EMS steel plate and after performing the LPR tests.
3. Measuring moisture content at incremental depths in the thick concrete slab underneath the metal plate and two walls. All moisture content measurements shall be made using a GE Protimeter™ with an auxiliary deep-wall probe at various locations on the floor near selected locations where core samples will be extracted. The technique uses a two-wire probe to measure the concrete resistivity which is inversely related to the moisture content. A series of moisture measurements were made using the Protimeter probe, and a moisture profile was obtained. This test was performed prior to removing the core samples.

1.3.4 Task 4

Analyze the on-site in situ test results and prepare an interim report, which was submitted by ERDC to USACE-NAU on 9 September 2012. The interim report contained a clear summary of conclusive findings on the corrosion mechanism and the expected service life of the steel plates.

2 Field Testing the Experimental Plan

Task 1 included a review of available information on existing conditions and issues, and development of a field and laboratory testing plan. The required steps for performing the in-situ LPR corrosion rate measurements and the corrosion potential measurements were developed based on verbal and emailed descriptions of the structure construction. These seven steps are outlined below.

Step 1: Drill 4 in. core through concrete liner to steel plate EMS using diamond core drill (Figure 1).

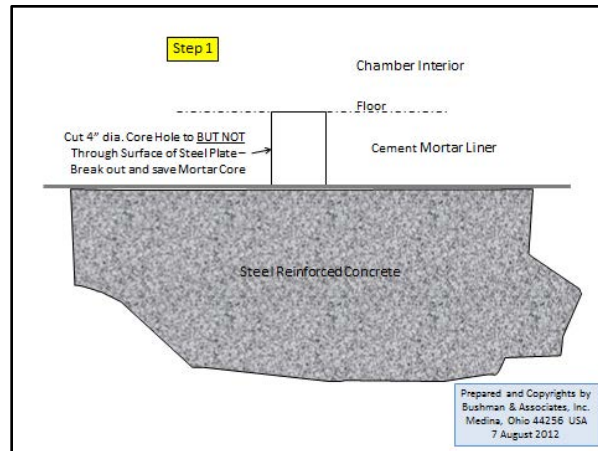


Figure 1. Step 1 of the in-situ LPR corrosion rate measurements.

Step 2: Pin EMS steel plate to underlying reinforced concrete with steel bolts inserted through EMS into epoxy-filled holes (Figure 2).

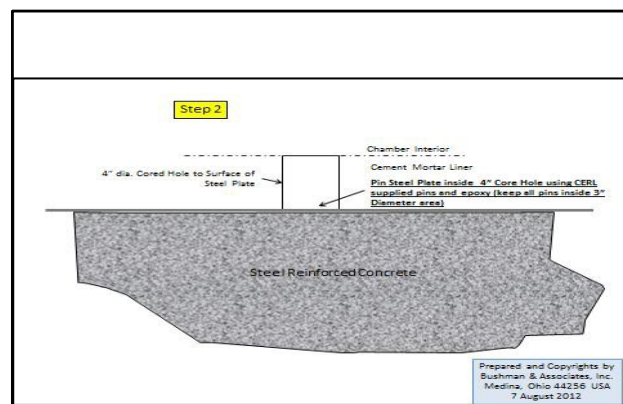


Figure 2. Step 2 of the in-situ LPR corrosion rate measurements.

Step 3: After bolt epoxy has cured, use 3 in. diameter diamond-tipped core drill to drill down through steel plate and at least 2 ½ in. into underlying concrete (Figure 3). Be sure drill is centered on the bolts securing the plate to concrete.

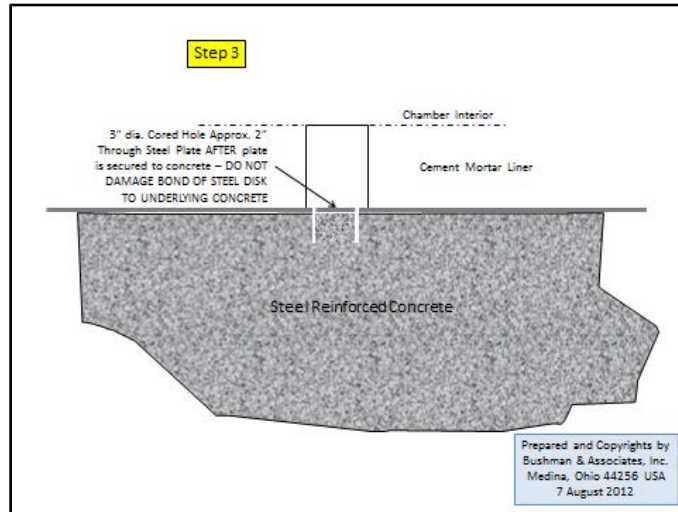


Figure 3. Step 3 of the in-situ LPR corrosion rate measurements.

Step 4: Insert precious metal oxide coated counter and reference electrodes into opposite sides of annulus created by 3 in. diameter core hole so that bottom of electrode touches the bottom of cored hole (Figure 4).

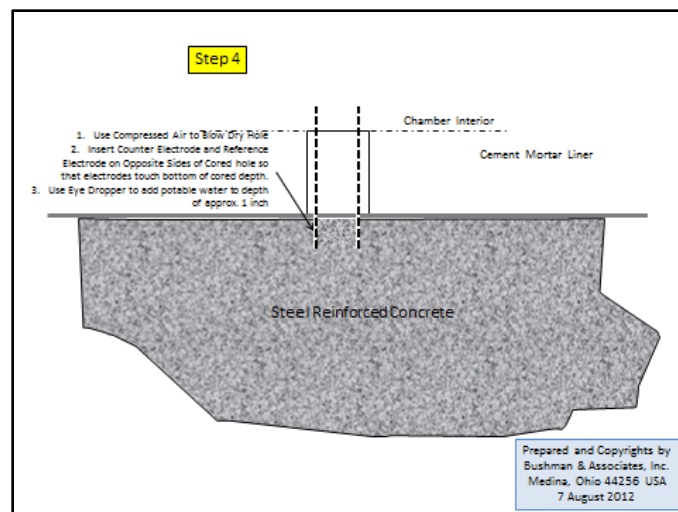


Figure 4. Step 4 of the in-situ LPR corrosion rate measurements.

Step 5: Connect Gamry test leads to counter (white lead) and reference electrodes (red lead) and blue/green leads to pointed tool pressed in contact with center disk (working electrode of 3 in. diameter steel EMS disk) (Figure 5). Be sure counter and reference electrode insulated section isolates electrodes from EMS plate.

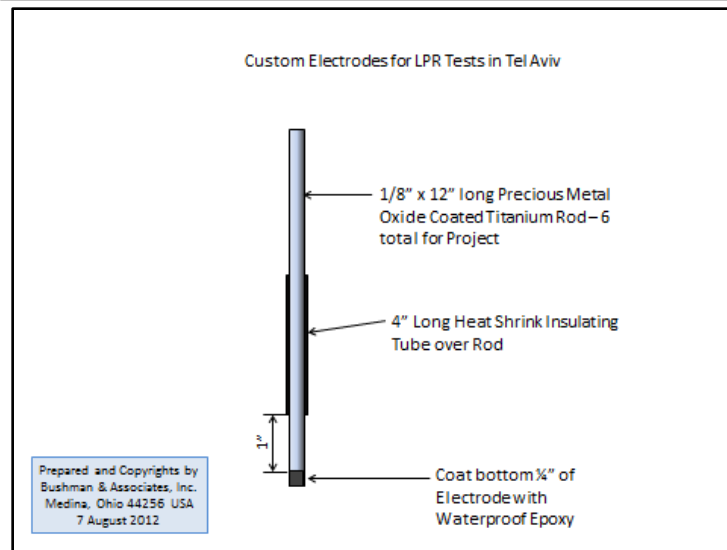
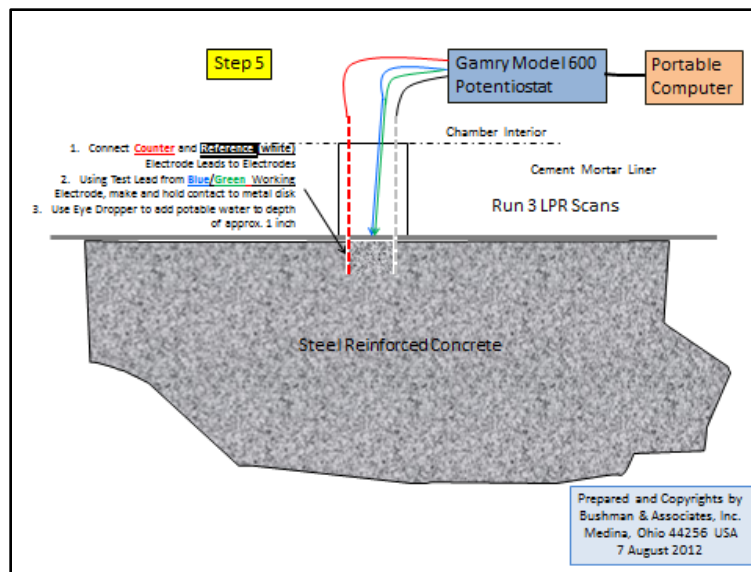


Figure 5. Step 5 of the in-situ LPR corrosion rate measurements.

Step 6: After LPR tests are complete (minimum 3 scans per cored hole), continue 3 in. core hole down to minimum 4–6 in. depth below EMS steel plate. Remove the breakout core from hole for future laboratory analysis by ERDC-CERL. After core is removed, detach EMS steel plate from core and exam surface in contact with underlying concrete (including photo

documentation) to define percentage of surface that is suffering corrosion attack (Figure 6).

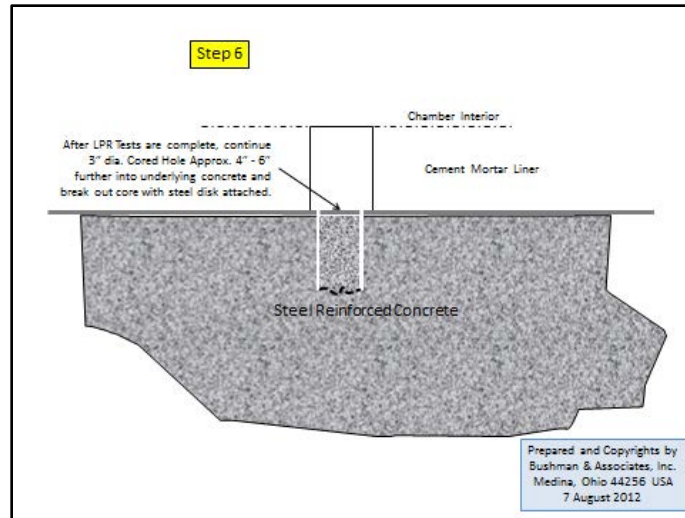


Figure 6. Step 6 of the in-situ LPR corrosion rate measurements.

Step 7: Measure steel EMS surface in contact with underlying concrete electrical corrosion potential using 3.5 molar potassium chloride/silver/silver chloride reference electrode and Fluke Model 289 5½ digit precision VOM meter (Figure 7).

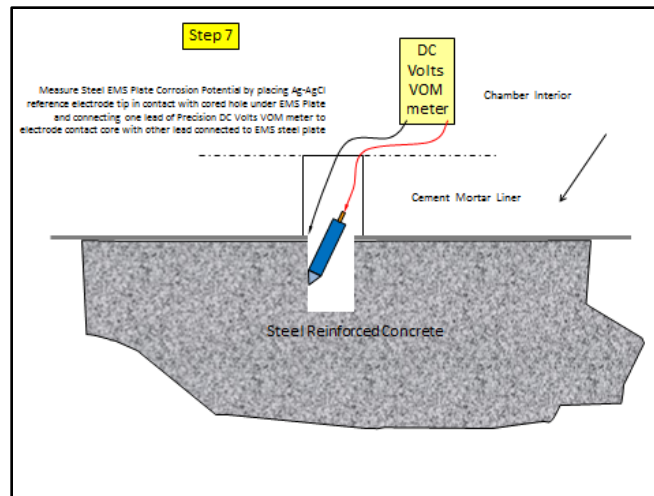


Figure 7. Step 7 of the in-situ LPR corrosion rate measurements.

3 Field Testing: August 9–17, 2012

The initial site inspection revealed that there were a number of approximately 16 in. (40 cm) wide troughs (Figure 8) that had been cut through the inner concrete liner to expose the EMS steel plate for inspection by others. It was decided that many of the test sites could be located within the pre-cut troughs, saving considerable work by the site contractor and allowing additional time to perform the testing.

It was also determined that the site contractor had the capability of readily cutting 16 in. (40 cm) diameter core holes down to the EMS plate (Figure 9) which then could be readily removed to expose the plate. These larger access ports would also make later testing more efficient and accurate.



Figure 8. Existing trough in concrete liner over EMS steel plate.



Figure 9. 16 in. diameter core hole cut to expose steel EMS for testing.

During this inspection, the general location of 10–12 test locations were identified on the main-floor level; it was anticipated that an additional two locations would be tested in the sunken portion of the floor, and two wall samples would also be tested (one near floor level and one near the ceiling). If time permitted, it was intended that one core would be taken in the ceiling, but it was later determined that the local contractor's equipment could not cut cores in the ceiling. This restriction was primarily because water cooling of the contractor's cutting tool was required, and this cutting solution would flow down on and into the electric motor driving the core drill. After the site inspection was completed, the testing plan was finalized including additional details for the work that would begin on Sunday morning, beginning at 8 a.m. that day and each day thereafter. It should be noted that each test day typically ended at 6 p.m., and lunch breaks were not taken.

The test equipment was unpacked on Saturday, before testing began; each piece of equipment including meter, reference electrode, camera, and test leads were individually tested for functionality and accuracy. The LPR system then was set up, and several full scans were completed using glass chambers containing the "working", "counter," and "reference" electrodes coupled to the Gamry 600 instrument. In turn, the Gamry 600 was connected to an HP Envy 15 portable computer equipped with the necessary LPR testing software.

An initial meeting was held on Sunday morning with local USACE and site contractor personnel¹ to familiarize all personnel with the study plans, methodologies, and assistance needed from M+W. M+W personnel indicated they were fully equipped to meet the project needs and would provide the necessary professional support staff to facilitate the project including coring all test holes, providing lighting for dark locations, vacuums and minimum 100 psi air pressure nozzle blasters to clean holes. Their assistance was essential to the successful completion of the project. Figure 10 shows the instrument cases being transported to the basement test site.

¹ M+W Group of M+W U.S., Inc. of Rehovot, Israel (M+W).

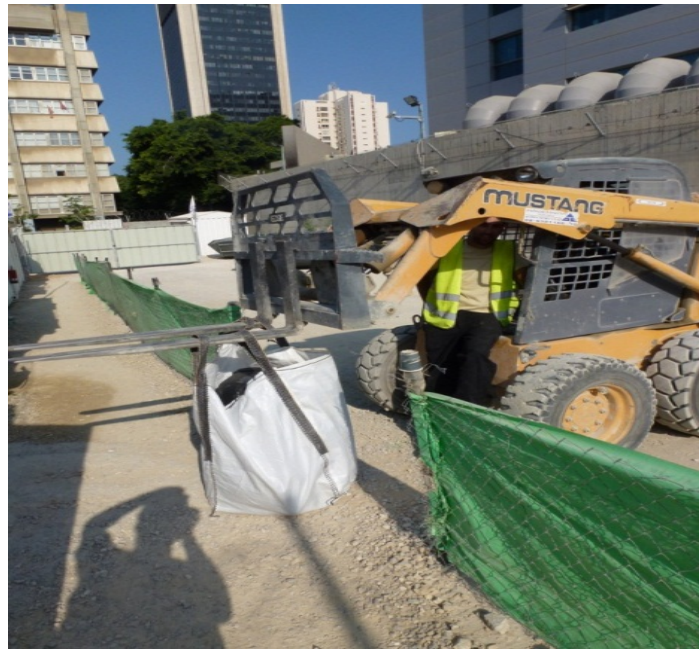


Figure 10. Synthetic canvas bag containing two large instrument cases for transport to basement test site.

It was then decided that trial LPR scans and concrete moisture tests should be performed at the first two locations to confirm the methodology to be used and to identify any problems. To perform the subsequent LPR testing, it was essential that the steel plate be held firmly in place while cutting through the plate with a core drill. To accomplish this, it was necessary to drill three 5/16 in. (0.8 cm) diameter holes approximately 1.5 in. (3.9 cm) deep through the steel plate on an equilateral triangle spacing to prevent the cut plate from rotating independent of the concrete cylinder as the diamond core bit rotated (see Step 2 of test procedure, Chapter 2). This proved to be extremely difficult as the EMS steel was an extremely hard material. Using drill bits with a titanium coating later improved the time to drill the three holes on each plate. After the three holes were drilled through the electromagnetic field (EMF) plate into the underlying concrete, the holes were first vacuum cleaned, followed by high-pressure air blowing to remove all dust and moisture (although moisture would immediately begin seeping back into these holes at some locations). Immediately following cleaning of each hole, a special caulking gun was placed into each hole; the gun contained two tubes of epoxy components (A & B) with a spiral mixing tip. Sufficient epoxy was injected to barely overflow each hole, immediately after which the steel bolts were firmly inserted flush to the plate in each hole (Figure 11–Figure 14). In most cases, the bolts had to

be depressed several times to displace enough epoxy so that the bolt head was tight to the steel plate.



Figure 11. Epoxy injection overview.



Figure 12. Two-part epoxy-mixing caulking gun.



Figure 13. Close-up photo of epoxy injection.



Figure 14. Close-up photo of holes after final placement of bolts.

After the epoxy had cured for at least 1 hr, a socket wrench was used to ensure each bolt was firmly cemented into the underlying concrete. Following setting of the bolts in locations #1 and #2, a concrete coring machine equipped with a 4.6 in. (11.6 cm) inside diameter, diamond-tipped core bit was set in place so that the core bit would not cut into any of the bolt heads. The machine was then secured in place, and the diamond bit was lowered to cut through the steel plate and into the underlying concrete to a depth of 2.5 in. (6 cm) below the EMF steel plate at locations #1 and #2.

A number of issues were identified and techniques were evaluated to determine the best means for obtaining quality data. One of the biggest problems encountered in obtaining data was the continuing ingress of groundwater seeping into the cored hole. This condition changed the water level on a continuing basis at many of the core test locations. Where this situation existed, an industrial vacuum cleaner with water/dust separator was used with a narrow channel hose tip to remove water, as best as possible, at a rate which would keep the water at a constant level below the EMS plate level.

4 Core Sample Testing

ERDC-CERL requested that the Concrete and Materials Branch (CMB) of ERDC-GSL provide support for the investigation of 16 of the 17 concrete core samples extracted from Site 81.² Appendix C shows the condition of the as-received core samples.

The thickness measurements of the two EMS steel plate sections that were shipped with the core samples were:

1. The floor section thickness was an average (three measurements) 0.116 inches (2.9464 mm).
2. The wall section thickness was an average (three measurements) 0.1233 inches (3.13 mm).

The thickness measurements indicate very little floor EMS plate metal loss over the 11-year timeframe since construction. This conclusion is based on the original EMS plate thickness of ~3 mm estimate by NAU. This validates our service life estimates of 200–500 years based on the in situ corrosion rates (See Chapter 5, Conclusions).

On 17 September 2012, the 16 concrete core samples were received by the CMB. Analyses requested for each sample included: (a) chloride content measurements at three depths from the surface of the core and (b) a general petrographic analysis of a polished sample to investigate key features of the concrete microstructure and any possible modes of deterioration present.

The following sections provide details of the techniques used for the chloride content and petrographic analysis and the results obtained.

² Author Vincent Hock verifies that 17 samples were taken at the site and none were mislabeled; however, he noted there was not a sample #2 received in the shipment of samples to ERDC-CERL, for which he supervised the unpacking. Thus, only 16 of the 17 samples originally taken could be analyzed.

4.1 Methods

4.1.1 Acid-soluble chloride content analysis

An analysis of acid-soluble chloride content was performed according to ASTM C1152, "Standard Test Method for Acid-Soluble Chloride in Mortar and Concrete." Segments of concrete were sectioned from each core at depths of 0–1 in., 1–2 in., and 2–3 in. from the surface of the core. Embedded pieces of rebar in the segments were removed by rough crushing of concrete in a hydraulic press. Each concrete segment was pulverized until it would pass through a No. 20 sieve (850 μm). Acid-soluble chloride was extracted from 10 g of the pulverized concrete powder by first dispersing the powder in 100 ml of deionized water (H_2O), followed by addition of 25 ml solution of dilute nitric acid (HNO_3 at 1:1 with deionized H_2O). Solutions were then filtered and stored in vials.

Chloride content analysis was performed using ion chromatography by the Environmental Chemistry Branch of the ERDC Environmental Laboratory (ERDC-EL). Results of chloride content analyses were provided as parts per million (ppm) in the solutions analyzed which was converted to a percentage by mass of the 10 g starting material. This percentage by mass value was then converted to typical lb/yd^3 and kg/m^3 by using assumed concrete unit weights of $4000 \text{ lb}/\text{yd}^3$ and $2400 \text{ kg}/\text{m}^3$, respectively.

4.1.2 Petrographic analysis

Petrographic analysis using stereomicroscopy (SM) was performed on all samples according to ASTM C856, "Standard Practice for Petrographic Examination of Hardened Concrete." An approximately 1 in. thick slice was made from each concrete core received and lapped using alumina suspensions in water to a particle size of 5 μm . Polished samples were imaged using a Zeiss Stereo Discovery V12 microscope at magnifications of 5x–15x. An overall image was taken of each sample at low magnification and at least three selected sites were also imaged at higher magnification. Key microstructural features noted included fine and coarse aggregate size, morphology and mineralogy, air voids, the presence of fibers, and any deterioration observed.

4.2 Results and discussion

4.2.1 Acid-soluble chloride content

Results from acid-soluble chloride analysis are presented in Table 1 and Table 2 for each of the sixteen concrete cores at 0–1 in., 1–2 in., and 2–3 in. depths from the surface. Chloride content ranges from 0.097–2.068 lb/yd³. However, all but the topmost layer in sample #1 were below the threshold limit of 1 to 2 lbs/yd³ of concrete necessary to initiate corrosion. 11 of the 16 cores tested had no definable increase in chloride ion concentration from the 3 in. level up through the 2 in. level to the 1 in. depth. Because the GSL team had no knowledge of the configuration and location of concrete cores taken at Site 81, conclusions related to potential exposure conditions and chloride ingress trends could not be made. Reinforcing bars extracted from cores showed signs of minor corrosion (Figure 15); however, this condition most likely was due to atmospheric corrosion prior to or during original installation of the rebar. Corrosion of the reinforcing steel's exposed surface at the exterior of concrete cores was also noted; however, such corrosion likely occurred following the coring process when the steel was exposed to neutral pH water and oxygen.



Figure 15. Segments of reinforcing steel extracted at 2-3 in. depth from core sample #4 (left) and core sample #5 (right) with both showing minor surface corrosion.

Table 1. Chloride content results from core samples #1–#11.

Core Sample No.*	Depth	Cl Content (%) *by mass concrete	Cl ⁻ Content (lb/yd ³) *assume 4000 lb/yd ³	Cl ⁻ Content (kg/m ³) *assume 2400 kg/m ³
#1	0-1 in.	0.052	2.068	1.228
	1-2 in.	0.039	1.540	0.914
	2-3 in.	0.027	1.060	0.629
#3	0-1 in.	0.023	0.924	0.549
	1-2 in.	0.007	0.289	0.171
	2-3 in.	0.009	0.364	0.216
#4	0-1 in.	0.021	0.831	0.493
	1-2 in.	0.008	0.336	0.199
	2-3 in.	0.004	0.179	0.106
#5	0-1 in.	0.007	0.281	0.167
	1-2 in.	0.003	0.116	0.069
	2-3 in.	0.003	0.123	0.073
#6	0-1 in.	0.012	0.467	0.277
	1-2 in.	0.008	0.321	0.190
	2-3 in.	0.009	0.357	0.212
#7	0-1 in.	0.020	0.818	0.486
	1-2 in.	0.016	0.639	0.380
	2-3 in.	0.009	0.354	0.210
#8	0-1 in.	0.017	0.669	0.397
	1-2 in.	0.013	0.506	0.300
	2-3 in.	0.011	0.428	0.254
#9	0-1 in.	0.007	0.300	0.178
	1-2 in.	0.006	0.220	0.131
	2-3 in.	0.005	0.207	0.123
#10	0-1 in.	0.004	0.163	0.097
	1-2 in.	0.007	0.279	0.166
	2-3 in.	0.008	0.332	0.197
#11	0-1 in.	0.015	0.595	0.353
	1-2 in.	0.011	0.454	0.270
	2-3 in.	0.008	0.322	0.191

*Note: sample #2 was not included in this study due to not being included in shipment.

Table 2. Chloride content results from core samples #12–#17.

Core Sample No.	Depth	Cl Content (%) *by mass concrete	Cl ⁻ Content (lb/yd ³) *assume 4000 lb/yd ³	Cl ⁻ Content (kg/m ³) *assume 2400 kg/m ³
#12	0-1 in.	0.008	0.316	0.187
	1-2 in.	0.007	0.294	0.175
	2-3 in.	0.006	0.221	0.131
#13	0-1 in.	0.005	0.186	0.110
	1-2 in.	0.002	0.097	0.058
	2-3 in.	0.003	0.121	0.072
#14	0-1 in.	0.005	0.199	0.118
	1-2 in.	0.003	0.121	0.072
	2-3 in.	0.003	0.127	0.075
#15	0-1 in.	0.005	0.212	0.126
	1-2 in.	0.003	0.136	0.081
	2-3 in.	0.005	0.189	0.112
#16	0-1 in.	0.003	0.130	0.077
	1-2 in.	0.004	0.142	0.085
	2-3 in.	0.003	0.124	0.074
#17	0-1 in.	0.005	0.205	0.122
	1-2 in.	0.005	0.196	0.117
	2-3 in.	0.005	0.205	0.121

4.2.2 Petrographic analysis

Selected representative images of each core sample are presented here. Additional photomicrographs of the same core samples are presented in Appendix D.

4.2.2.1 Core sample #1

Images of concrete from core sample #1 are shown in Figure 16. The concrete appears to be composed of an angular coarse and subangular-shaped fine aggregate of unknown composition. There appears to be very little air in the concrete. The concrete appears quite competent, with no visible cracks or signs of chemical reactions.

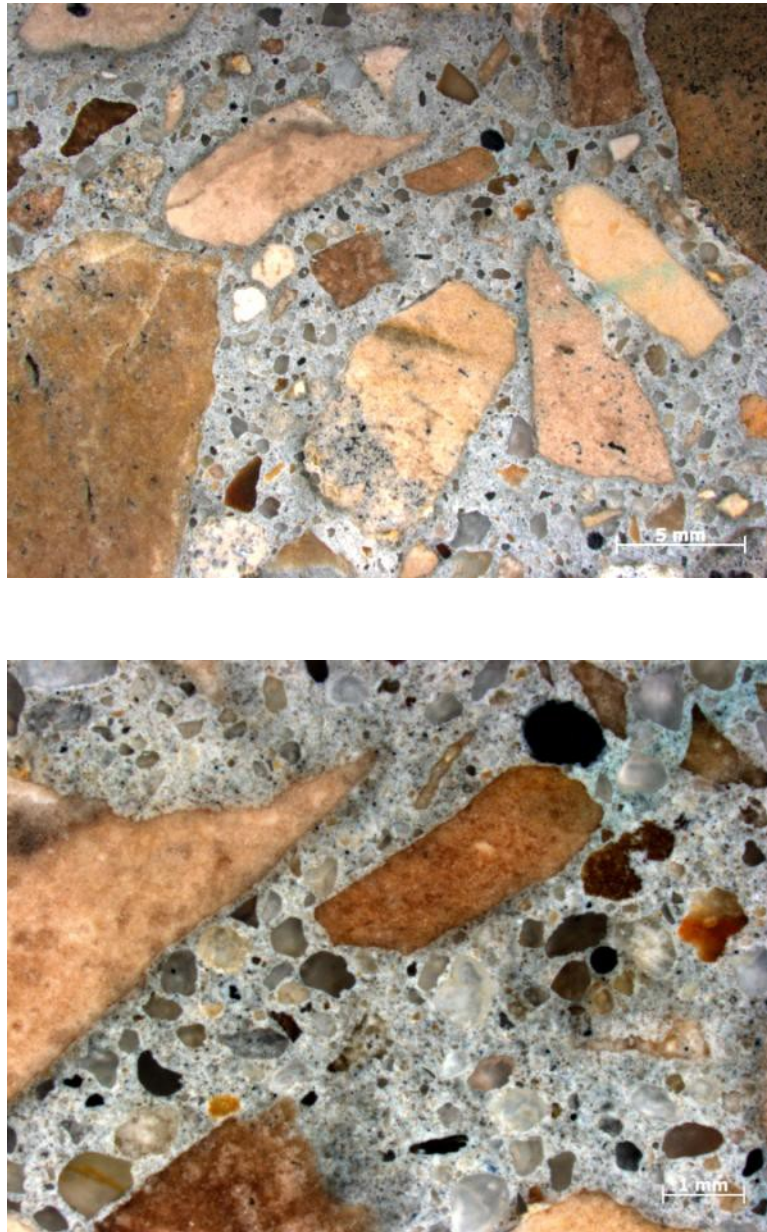


Figure 16. Photomicrographs of core sample #1 (5x above; 15x below).

4.2.2.2 Core sample #2

Core sample #2 was not included in this study due to its non-receipt in shipment to ERDC-CERL.

4.2.2.3 Core sample #3

Images of concrete from core sample #3 are shown in Figure 17. The concrete appears to be composed of an angular coarse and subangular-shaped fine aggregate of unknown composition. There appears to be very little air in the concrete. Although the concrete appears competent with no visible cracks, there are areas in the cement paste around selected aggregate particles that are lighter in color than the surrounding paste.

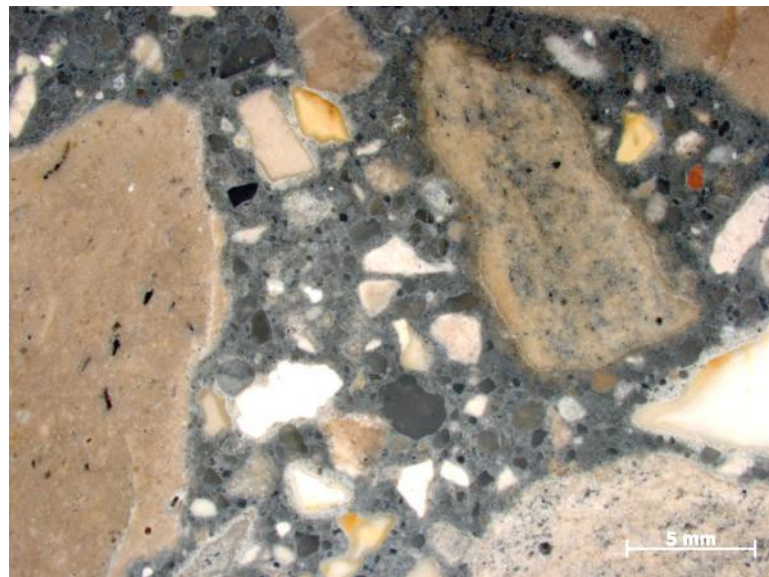


Figure 17. Photomicrographs of core sample #3 (5x above; 15x below).

4.2.2.4 Core sample #4

Images of concrete from core sample #4 are shown in Figure 18. The concrete appears to be composed of an angular coarse and subangular-shaped fine aggregate of unknown composition. Some entrapped air is visible in the concrete. The concrete appears quite competent, with no visible cracks or signs of chemical reactions.

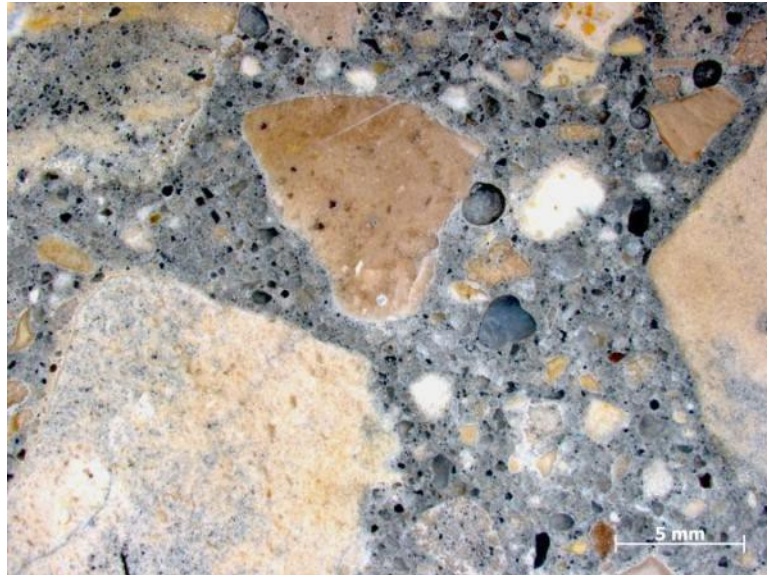


Figure 18. Photomicrographs of core sample #4 (5x above, 15x below).

4.2.2.5 Core sample #5

Images of concrete from core sample #5 are shown in Figure 19. The concrete appears to be composed of an angular coarse and subangular-shaped fine aggregate of unknown composition. There appears to be very little air in the concrete. Although the concrete appears competent with no visible cracks, there are areas in the cement paste around selected aggregate particles that are lighter in color than the surrounding paste.

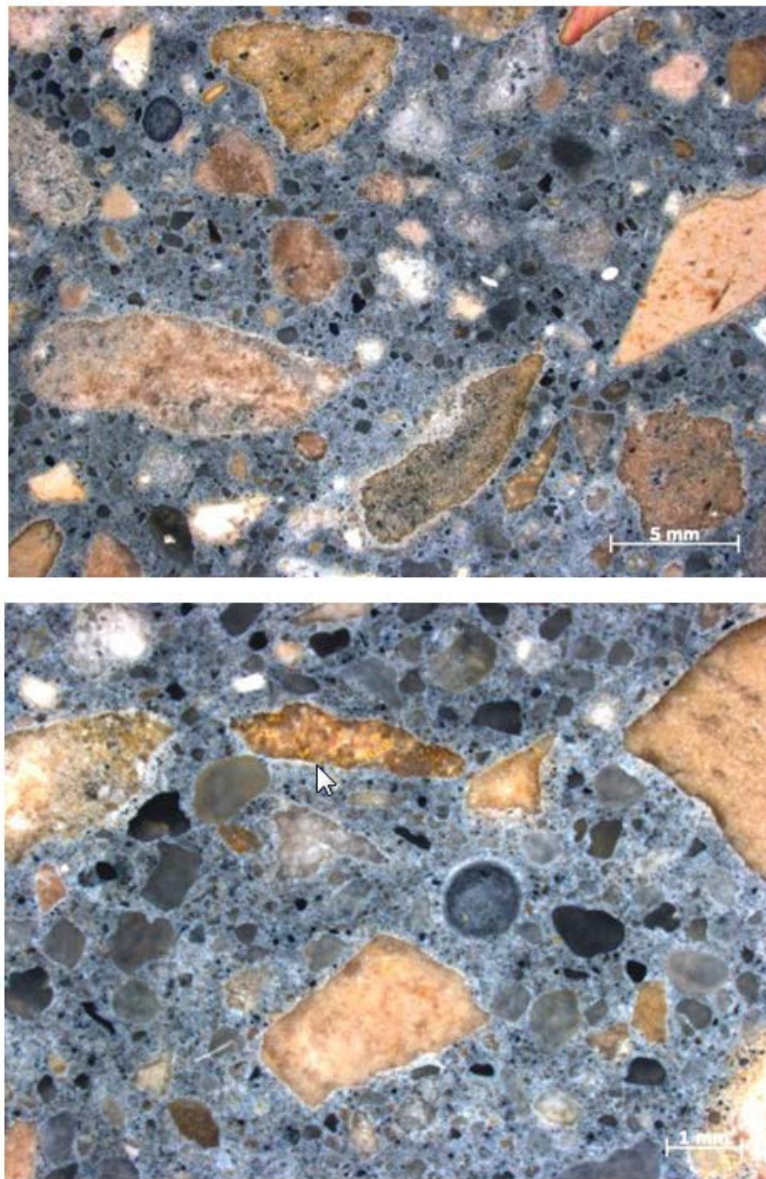


Figure 19. Photomicrographs of core sample #5 (5x above, 15x below).

4.2.2.6 Core sample #6

Images of concrete from core sample #6 are shown in Figure 20. The concrete appears to be composed of an angular coarse and subangular-shaped fine aggregate of unknown composition. There appears to be very little air in the concrete. The concrete appears quite competent, with no visible cracks or signs of chemical reactions.



Figure 20. Photomicrographs of core sample #6 (5x above, 15x below).

4.2.2.7 Core sample #7

Images of concrete from core sample #7 are shown in Figure 21. The concrete appears to be composed of an angular coarse and subangular-shaped fine aggregate of unknown composition. There appears to be very little air in the concrete. The concrete appears quite competent, with no visible cracks or signs of chemical reactions.

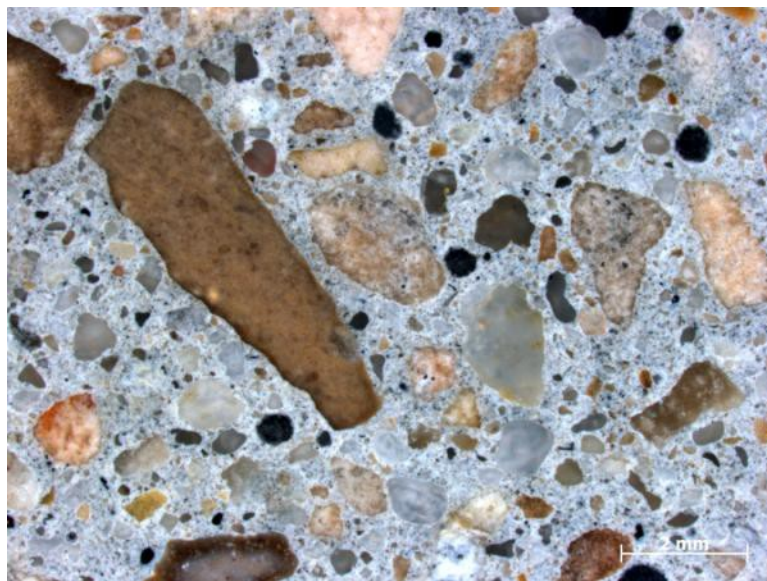
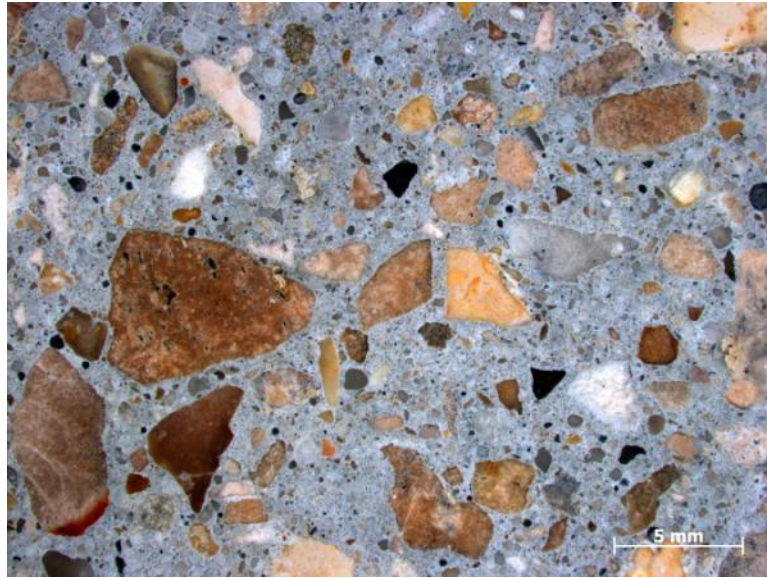


Figure 21. Photomicrographs of core sample #7 (5x above, 15x below).

4.2.2.8 Core sample #8

Images of concrete from core sample #8 are shown in Figure 22. The concrete appears to be composed of an angular coarse and subangular-shaped fine aggregate of unknown composition. There appears to be very little air in the concrete. The concrete appears quite competent, with no visible cracks or signs of chemical reactions.

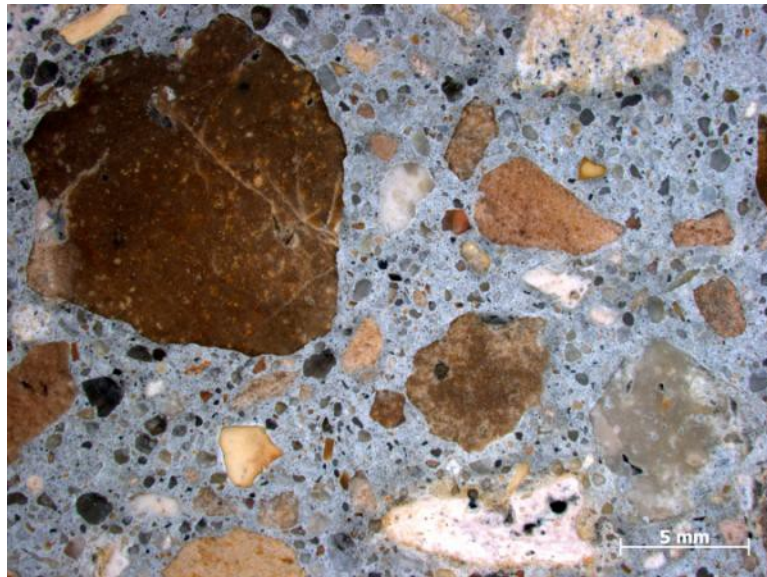


Figure 22. Photomicrographs of core sample #8 (5x above, 15x below).

4.2.2.9 Core sample #9

Images of concrete from core sample #9 are shown in Figure 23. The concrete appears to be composed of an angular coarse and subangular-shaped fine aggregate of unknown composition. There appears to be very little air in the concrete. The concrete appears quite competent, with no visible cracks or signs of chemical reactions.

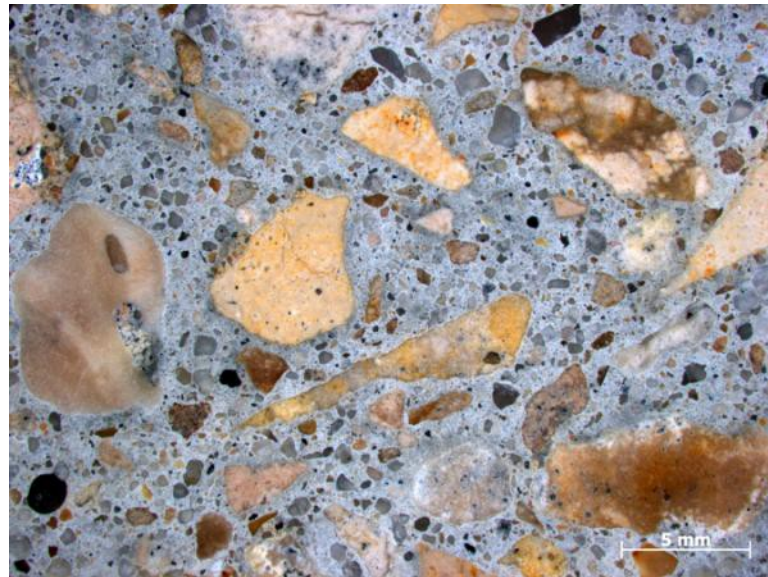


Figure 23. Photomicrographs of core sample #9 (5x above, 15x below).

4.2.2.10 Core sample #10

Images from core sample #10 are shown in Figure 24. The concrete appears to be composed of an angular coarse and subangular-shaped fine aggregate of unknown composition. There appears to be very little air in the concrete. A large crack in the concrete starts at the upper right center and proceeds through an orange-colored aggregate that extends into the cement paste. There are no indications of any chemical reactions, which may indicate the damage is due to application of some structural load.

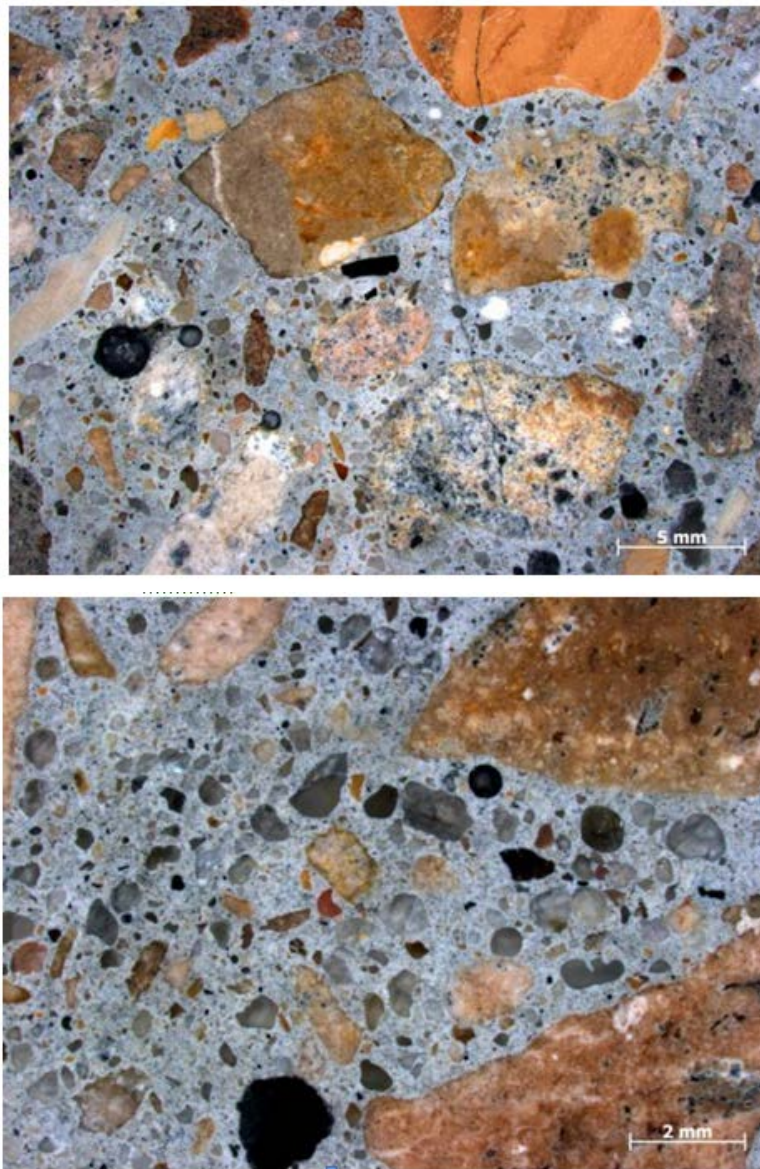


Figure 24. Photomicrographs of core sample #10 (5x above, 15x below).

4.2.2.11 Core sample #11

Images of concrete from core sample #11 are shown in Figure 25. The concrete appears to be composed of an angular coarse and subangular-shaped fine aggregate of unknown composition. There appears to be very little air in the concrete. The concrete appears quite competent, with no visible cracks or signs of chemical reactions.

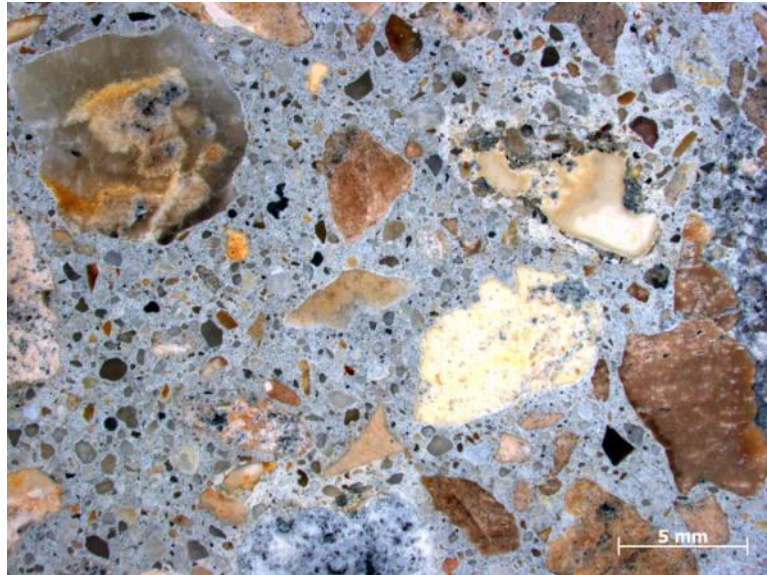


Figure 25. Photomicrographs of core sample #11 (5x above, 15x below).

4.2.2.12 Core sample #12

Images of concrete from core sample #12 are shown in Figure 26. The concrete appears to be composed of an angular coarse and subangular-shaped fine aggregate of unknown composition. There appears to be very little air in the concrete. The concrete appears quite competent, with no visible cracks or signs of chemical reactions.

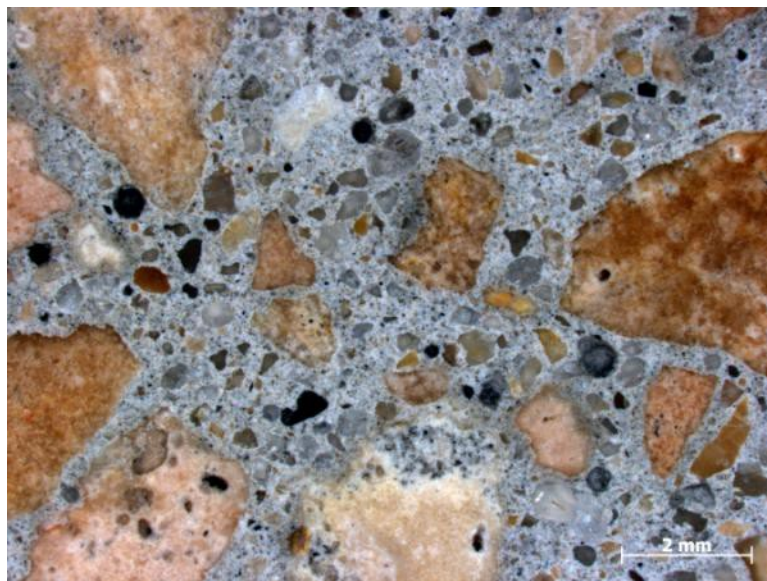
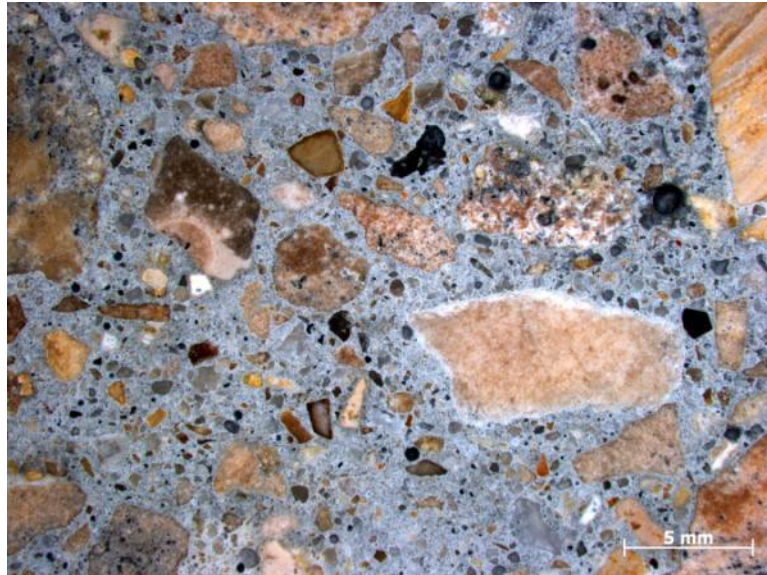


Figure 26. Photomicrographs of core sample #12 (5x above, 15x below).

4.2.2.13 Core sample #13

Images of concrete from core sample #13 are shown in Figure 27. The concrete appears to be composed of an angular coarse and subangular-shaped fine aggregate of unknown composition. There appears to be very little air in the concrete. The concrete appears quite competent, with no visible cracks or signs of chemical reactions.

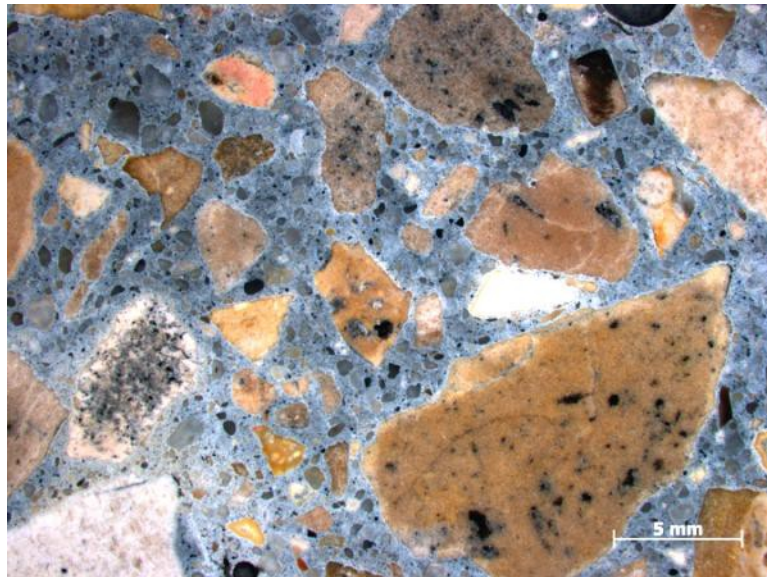


Figure 27. Photomicrographs of core sample #13 (5x above, 15x below).

4.2.2.14 Core sample #14

Images of concrete from core sample #14 are shown in Figure 28. The concrete appears to be composed of an angular coarse and subangular-shaped fine aggregate of unknown composition. There appears to be very little air in the concrete. The concrete appears quite competent, with no visible cracks or signs of chemical reactions.

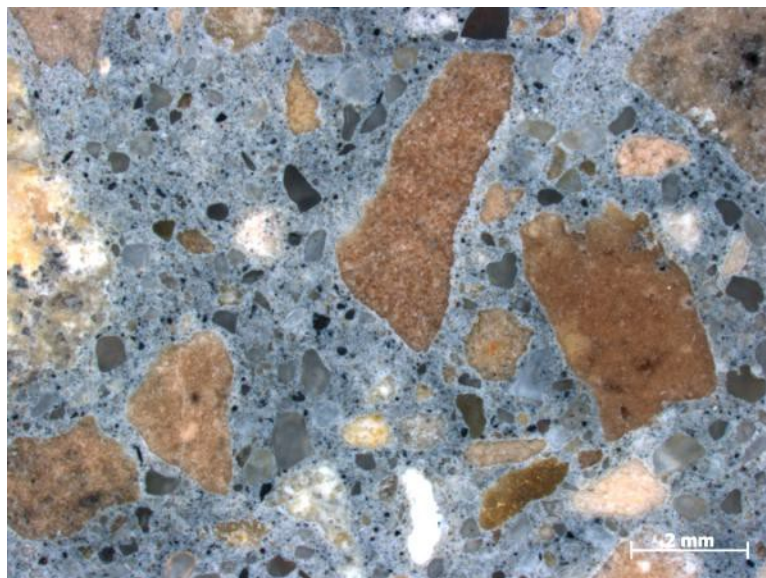
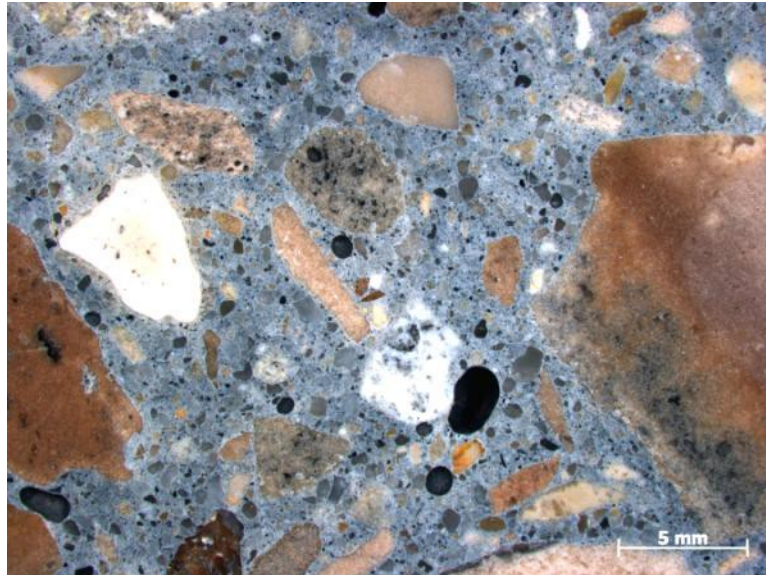


Figure 28. Photomicrographs of core sample #14 (5x above, 15x below).

4.2.2.15 Core sample #15

Images of concrete from core sample #15 are shown in Figure 29. The concrete appears to be composed of an angular-to-rounded coarse and subangular-to-rounded shaped fine aggregate of unknown composition. Steel fibers are present in the concrete. There appears to be very little air in the concrete. Although the concrete appears competent with no visible cracks, there are areas in the cement paste around selected aggregate particles that are lighter in color than the surrounding paste.

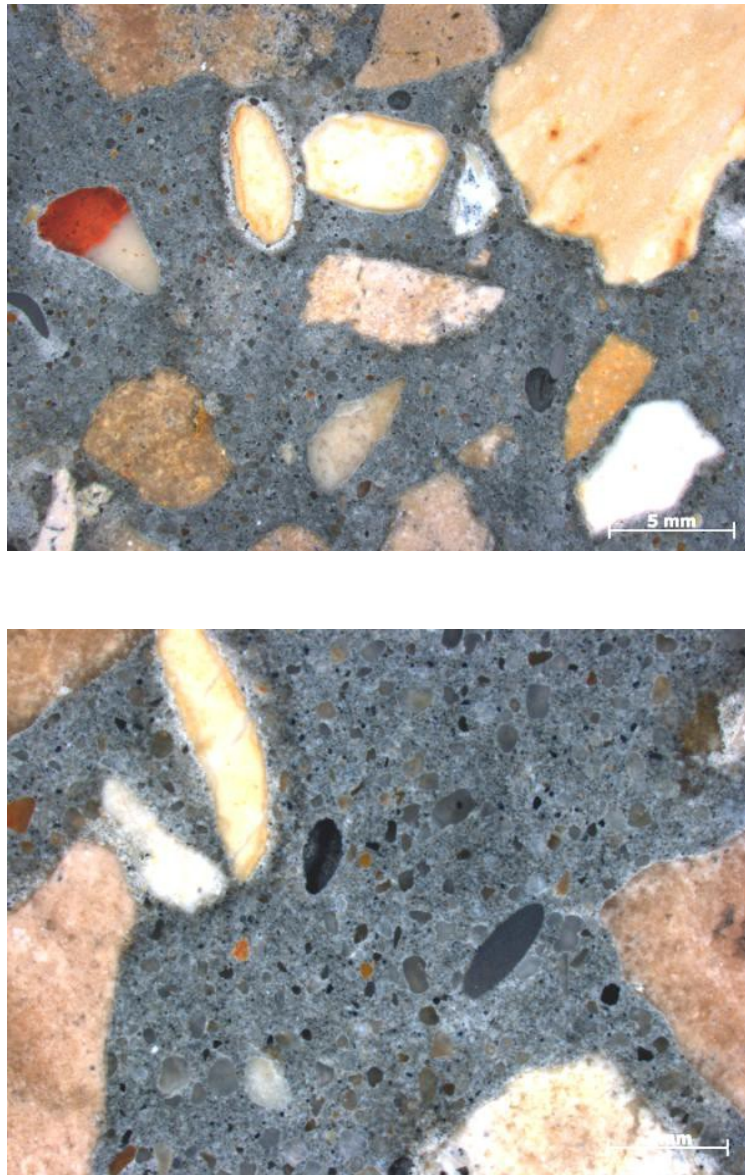


Figure 29. Photomicrographs of core sample #15 (5x above, 15x below).

4.2.2.16 Core sample #16

Images of concrete from core sample #16 are shown in Figure 30. The concrete appears to be composed of an angular coarse and subangular-shaped fine aggregate of unknown composition. There appears to be very little air in the concrete. The concrete appears quite competent, with no visible cracks or signs of chemical reactions.

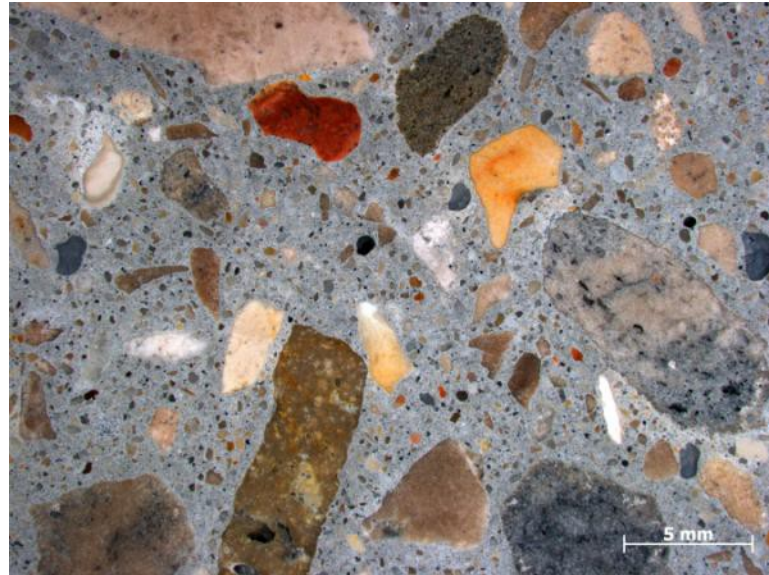


Figure 30. Photomicrographs of core sample #16 (5x above, 15x below).

4.2.2.17 Core sample #17

Images of concrete from core sample #17 are shown in Figure 31. The concrete appears to be composed of an angular-to-subangular coarse and subangular-to-rounded shaped fine aggregate of unknown composition. Steel fibers are present in the concrete. There appears to be very little air in the concrete. The concrete appears quite competent, with no visible cracks or signs of chemical reactions.



Figure 31. Photomicrographs of core sample #17 (5x above, 15x below).

4.3 Conclusions of concrete core testing

Sixteen concrete core samples from Site 81 were investigated from the 17 samples taken. The study of these core samples consisted of chloride content measurements at three depths from the surface and a petrographic analysis to identify key microstructural features and potential modes of deterioration. Conclusions from the study of the core samples are given below.

- Chlorides were found to be present in measureable quantities in each core analyzed, with contents ranging from 0.097–2.068 lb/yd³. Chloride contents in all but sample #1 were below the level of approximately 1–1.5 lb/yd³ of concrete necessary for initiation of corrosion of the embedded reinforcing steel. Further, Chloride contents generally did not decrease with depth from the surface. No corrosion was evident on reinforcing steel bars and fibers extracted from concrete cores during the crushing process.
- Petrographic examination of the 16 concrete samples investigated showed competent concrete. The coarse and fine aggregate appear to be suitable for concrete and appear to be well distributed. There were steel fibers present in two of the concrete specimens. There appeared to be very little air in any of the concrete samples. Although one concrete sample had a crack present, it did not appear that it was the result of any deleterious chemical reaction. Three samples had lightly-colored cement paste surrounding selected aggregate particles. The cause for this discoloration is unclear, but there does not appear to be any obvious deterioration or cracking occurring in those samples. The concrete appears quite competent, with no visible cracks or signs of chemical reactions.

5 Summary of Results

The corrosion rates measured were both extremely low and relatively uniformly distributed across the underlying surface of each cored EMS steel plate (17 cores total). The average of all corrosion rates measured was 0.2356 mils per year (0.005984 mm/year) as shown in Appendix B. Given an EMS steel plate original thickness of 125 mils (3.175 mm), the average time to penetration would be 530 years.

As stated previously, the thickness measurements of the two EMS steel plate sections that were shipped with the core samples were 0.116 inches (2.9464 mm) for the floor section thickness and 0.1233 inches (3.13 mm) for the wall section (both an average of three measurements). These thickness measurements indicate very little floor EMS plate metal loss over the 11-year timeframe since construction, based on the original EMS plate thickness of ~3 mm estimated by NAU. This validates our service life estimates of 200–500 years based on the in-situ corrosion rates.

In order to predict the worst case scenario with 95% confidence, the worst case corrosion rate including two standard deviations of the average values measured would be 0.6272 mils per year (0.01593 mm/year) providing a minimum expected life until first penetration of 199 years given the same original plate thickness of 125 mils (3.175 mm).

A review of the percent moisture content data as measured by the Protometer instrument at multiple levels in the core holes indicated that the concrete slab beneath the EMS steel plate was saturated with groundwater. The groundwater seepage was confirmed by ever-rising water levels in both the bolt and core holes. However, the presence of the groundwater which has saturated or nearly saturated the concrete slab does not promote corrosion of the EMS steel plate. This lack of corrosion is primarily due to lack of oxygen; oxygen was consumed by the initial corrosion of the plate shortly after construction, and oxygen replenishment is prevented by the presence of the steel EMS plate covering the concrete slab.

Analysis of the chloride ion concentration in the concrete core samples confirmed that the chlorides did not impact the corrosion rate of the EMS.

Further, the analyses of the groundwater samples (Appendix A) confirmed that the chlorides also did not impact the corrosion rate of the EMS.

6 Recommendations

Where the steel EMS steel plate has already been exposed, it is recommended that the exposed surfaces be cleaned using effective surface preparation methods and coated using the current practices. No further excavation of the steel EMS is recommended, since there was never any significant corrosion observed in the circular excavations made during this study. Further, the corrosion observed and examined at the floor/wall interface was minimal. Where the EMS steel plate has been penetrated, either during saw cutting or core drilling, appropriate repair measures to facilitate welding new material to reseal the EMS must be accomplished.

7 References

Angst, U., B. Elsener, C. K. Larsen, and Ø. Vennesland. 2009. "Critical Chloride Content in Reinforced Concrete - A Review," *Cement and Concrete Research* 39 (12): 1122-1138.

ASTM C856: "Standard Practice for Petrographic Examination of Hardened Concrete," West Conshohocken, PA: American Society for Testing and Materials.

ASTM C1152: "Standard Test Method for Acid-Soluble Chloride in Mortar and Concrete," West Conshohocken, PA: American Society for Testing and Materials.

FIB. 1992. *Design Guide for Durable Concrete Structures*. ed. Comité Euro-International du Béton - Fédération Internationale du Béton, Lausanne, Switzerland. London: Thomas Telford, Ltd.

Appendix A: Water Testing

Figures A-1 and A-2 are reproductions of test results from Illinois State Water Survey analyses of two water samples collected at Site 81. Test point #1, level 5 is water from the core hole and test point #2, level 1 is groundwater.

Based on the comparison of the water qualities shown in Figures A-1 and A-2, the water sample taken from the core hole (test point #1, level 5) is groundwater with increased levels of sulfate, silica, sodium, potassium and total dissolved solids. The raw groundwater filtering through the Portland cement has dissolved these elements, causing their increase in the water sample taken from the core hole. The only exception is calcium and magnesium, which are somewhat decreased in the core hole water sample as compared to the groundwater sample but both contain moderate amounts of each element. The most important factor to note about the tests is the dramatic increase in alkalinity of the core hole water sample due to filtering through the highly alkaline concrete.

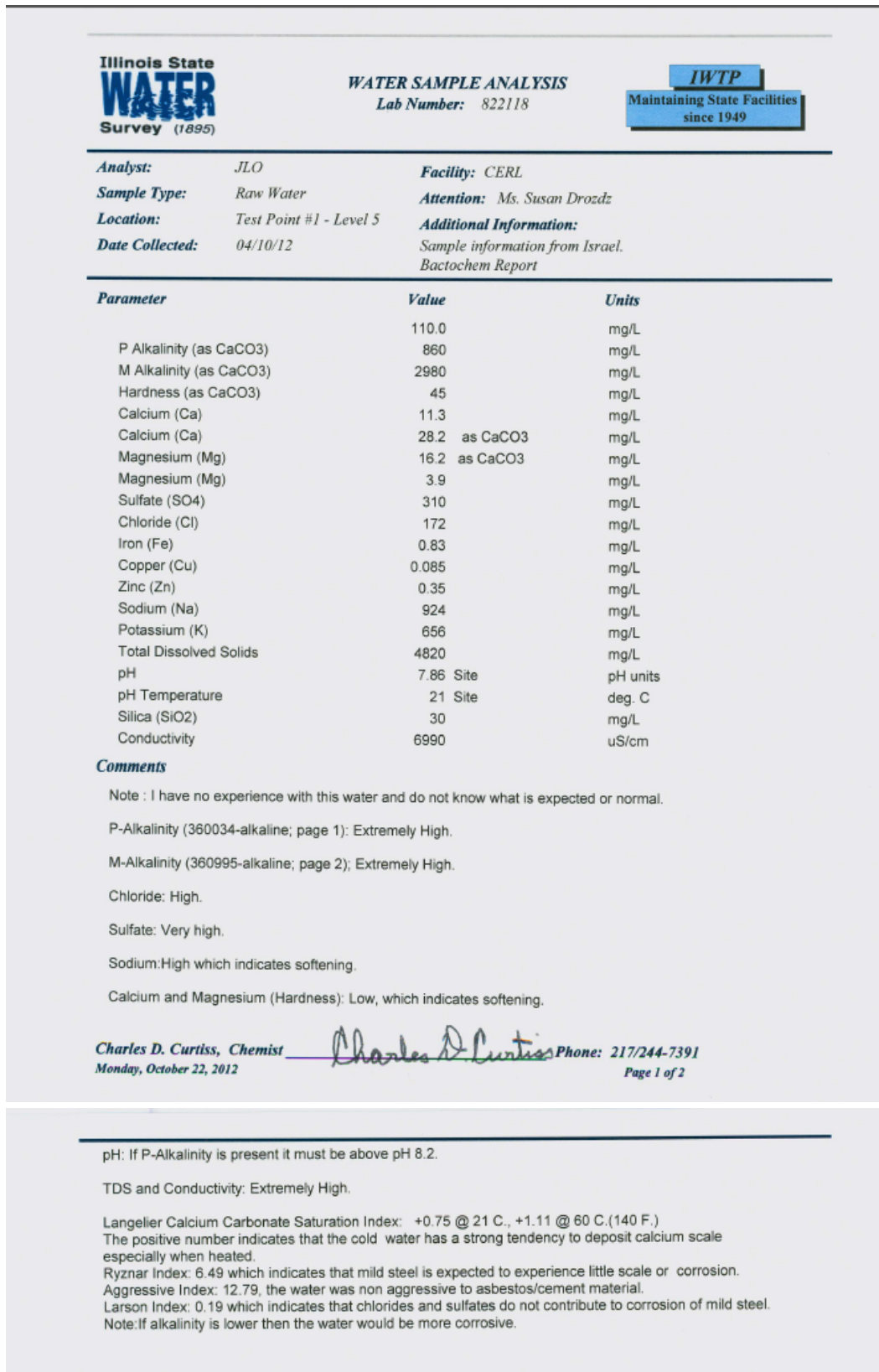


Figure A-1. Analysis of water sample taken from test point #1, level 5.

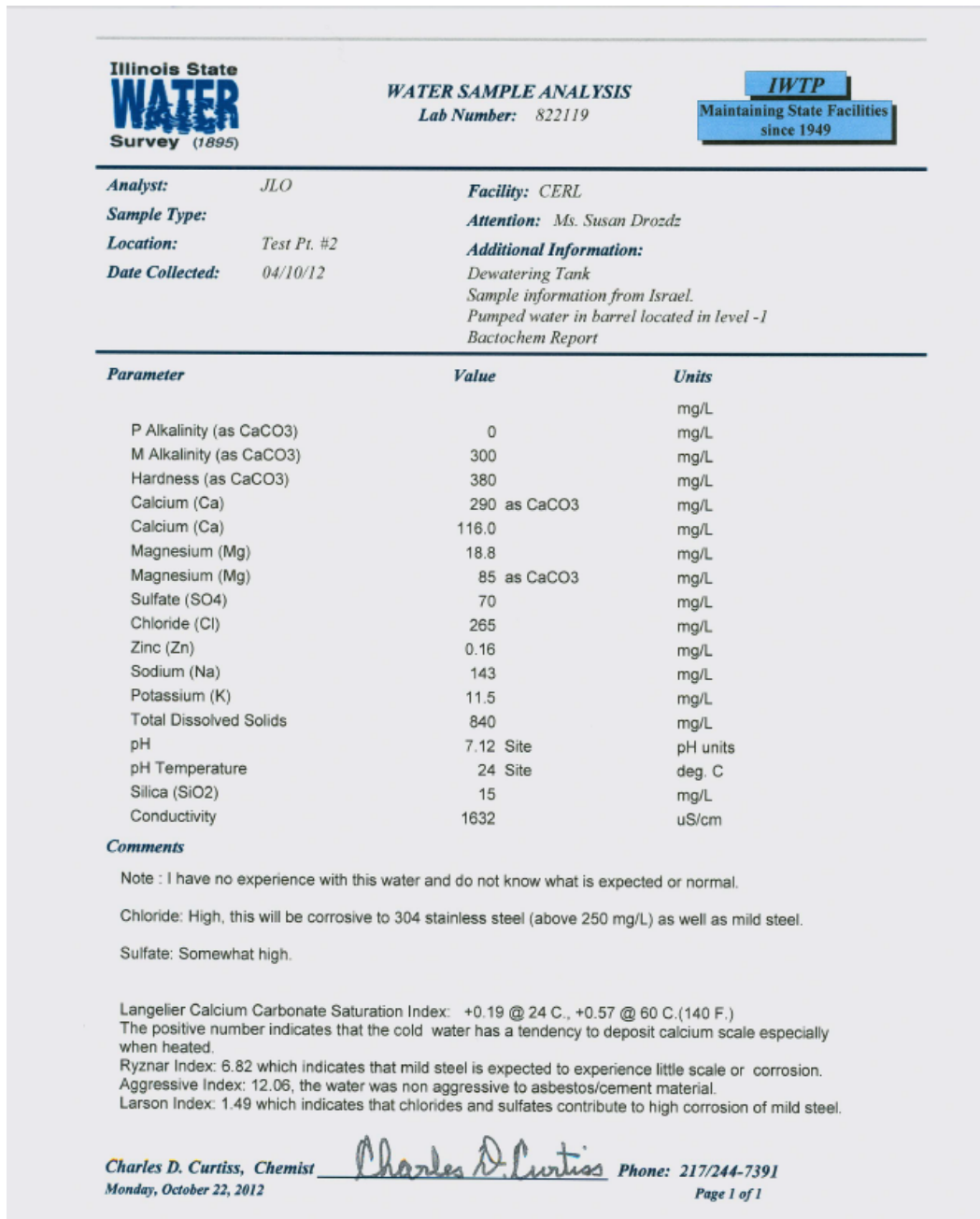


Figure A-2. Analysis of water sample taken from test point #2.

Appendix B: EMF Liner Corrosion Rate Measurement

Figures B-1 through B-4 represent the corrosion rate measurements for the 17 samples.

B&A Tel Aviv EMF Liner - Corrosion Rate Measurements							
Draft 0.98 - September 3, 2012							
Core No.	Scan	LPR Measured Corrosion Rate (mils/year)	Percent of Plate Estimated to be Actively Corroding	Average Corrosion Rate/Core (mils/year)	Comments	Percent Moisture Content on Protometer at 1", 2" and 3"	Corrosion Potential vs. Ag/AgCL/ 3.5 M KCl (-V)
1	A	0.01790	70%	0.02400	Water Rising in Cored Hole - Seeping in from Concrete	100%	0.566
1	B	0.01782			Seepage water is clear and is not from surface water	100%	
1	C	0.01467			100%		
2	A	0.12464	85%	0.09577		100%	0.560
2	B	0.05546			100%		
2	C	0.06411			100%		
3	A	0.39140	60%	0.66205		100%	0.493
3	B	0.39929			100%		
3	C	0.40100			100%		
4	A	0.06101	95%	0.05324		100%	0.572
4	B	0.03723			100%		
4	C	0.05350			100%		
5	A	0.13430	90%	0.15933	Fastest Rising Water - Vacuumed almost continuously	100%	0.515
5	B	0.14470			Fast Rising Water - Vacuumed almost continuously - Intermittent Vacuuming causes some "blips" in data but slopes ok	100%	
5	C	0.15120			Fastest Rising Water - Vacuumed almost continuously	100%	

Figure B-1. Corrosion rate measurements for core samples #1-5.

B&A Tel Aviv EMF Liner - Corrosion Rate Measurements							
Draft 0.98 - September 3, 2012							
Core No.	Scan	LPR Measured Corrosion Rate (mils/year)	Percent of Plate Estimated to be Actively Corroding	Average Corrosion Rate/Core (mils/year)	Comments	Percent Moisture Content on Protometer at 1", 2" and 3"	Corrosion Potential vs. Ag/AgCl/ 3.5 M KCl (-V)
6	A	0.05444	95%	0.11203	Fast Rising Water - Vacuumed almost continuously	100%	0.535
6	B	0.13590			Fast Rising Water - Vacuumed almost continuously - Intermittent Vacuuming causes some "blips" in data but slopes ok	100%	
6	C	0.12894			Fast Rising Water - Vacuumed almost continuously	100%	
7	A	0.61800	95%	0.65987		100%	0.548
7	B	0.61192				100%	
7	C	0.65071				100%	
8	A	0.52246	90%	0.50319	Water Rising	100%	0.547
8	B	0.63652			Water Rising too high	100%	
8	C	0.9106*			Water Rising too high ... at steel plate	100%	
8	D	0.19963			Water Level lowered	100%	
9	A	0.08091	80%	0.11444	Fast filling hole near wall - must continuously vacuum out water	100%	0.460
9	B	0.10870			Fast filling hole near wall - must continuously vacuum out water	100%	
9	C	0.08505			Fast filling hole near wall - must continuously vacuum out water	100%	
10	A	0.19140	100%	0.18196	Water Rising too high - reached plate at outlier data	100%	0.752
10	B	0.16952				100%	
10	C	0.18496			Break in curve caused by rising water vacuuming	100%	

Figure B-2. Corrosion rate measurements for core samples #6-10.

B&A Tel Aviv EMF Liner - Corrosion Rate Measurements							
Draft 0.98 - September 3, 2012							
Core No.	Scan	LPR Measured Corrosion Rate (mils/year)	Percent of Plate Estimated to be Actively Corroding	Average Corrosion Rate/Core (mils/year)	Comments	Percent Moisture Content on Protometer at 1", 2" and 3"	Corrosion Potential vs. Ag/AgCl/ 3.5 M KCl (-V)
11	A	0.31900	100%	0.33392	Fast filling hole - must continuously vacuum out water	100%	0.523
11	B	0.36050			Fast filling hole - must continuously vacuum out water	100%	
11	C	0.32225			Fast filling hole - must continuously vacuum out water	100%	
12	A	0.25354	100%	0.30454		100%	0.684
12	B	0.32979				100%	
12	C	0.33029				100%	
13	A	0.02729	90%	0.03488		100%	0.537
13	B	0.03302				100%	
13	C	0.03386				100%	
14	A	0.05103	80%	0.07618		100%	0.605
14	B	0.06486				100%	
14	C	0.06563				100%	
14	D	0.06226			Artificially overfilled slot to see impact on measurement	100%	
15	A	0.07414	40%	0.22588		41%	0.325
15	B	0.10950				41%	
15	C	0.08742				41%	

Figure B-3. Corrosion rate measurements for core samples #11-15.

B&A Tel Aviv EMF Liner - Corrosion Rate Measurements							
Draft 0.98 - September 3, 2012							
Core No.	Scan	LPR Measured Corrosion Rate (mils/year)	Percent of Plate Estimated to be Actively Corroding	Average Corrosion Rate/Core (mils/year)	Comments	Percent Moisture Content on Protometer at 1", 2" and 3"	Corrosion Potential vs. Ag/AgCl/ 3.5 M KCl (-V)
16	A	0.12660	50%	0.26113	Plate could not be separated from Concrete Core - JBB Estimated at 50% corroded for Calculation Purpose until CERL laboratory removes plate, measures and photo documents corroded area.	32%	0.237
16	B	0.12780				54%	
16	C	0.13730				78%	
17	A	0.17490	80%	0.20388	Artificially overfilled slot to see impact on measurement	36%	0.187
17	B	0.17500					
17	C	0.13940					
Average Percent of Plate Actively Corroding:			82%	0.23566			0.509
Minimum Corrosion Rate Measured:				0.01467			
Maximum Corrosion Rate Measured:				0.65071			
Std. Dev. of all Data:			17.3%	0.19577			0.139
Max. for 2 Std. Deviations of Average Corrosion Rates for Each Core:			100%	0.62721			0.786
Estimated Minimum Life in Years until 1st Penetration for 0.125" Wall Thickness Plate:				199			

Figure B-4. Corrosion rate measurements for core samples #16–17, and collective data for all samples.

Appendix C: As-Received Core Samples

Figures C-1 – C-16 represent the as-received core samples #1 and #3–#16. Again, note that core sample #2 is not included here, due to it not being received in the original shipment to the ERDC lab from Site 81.

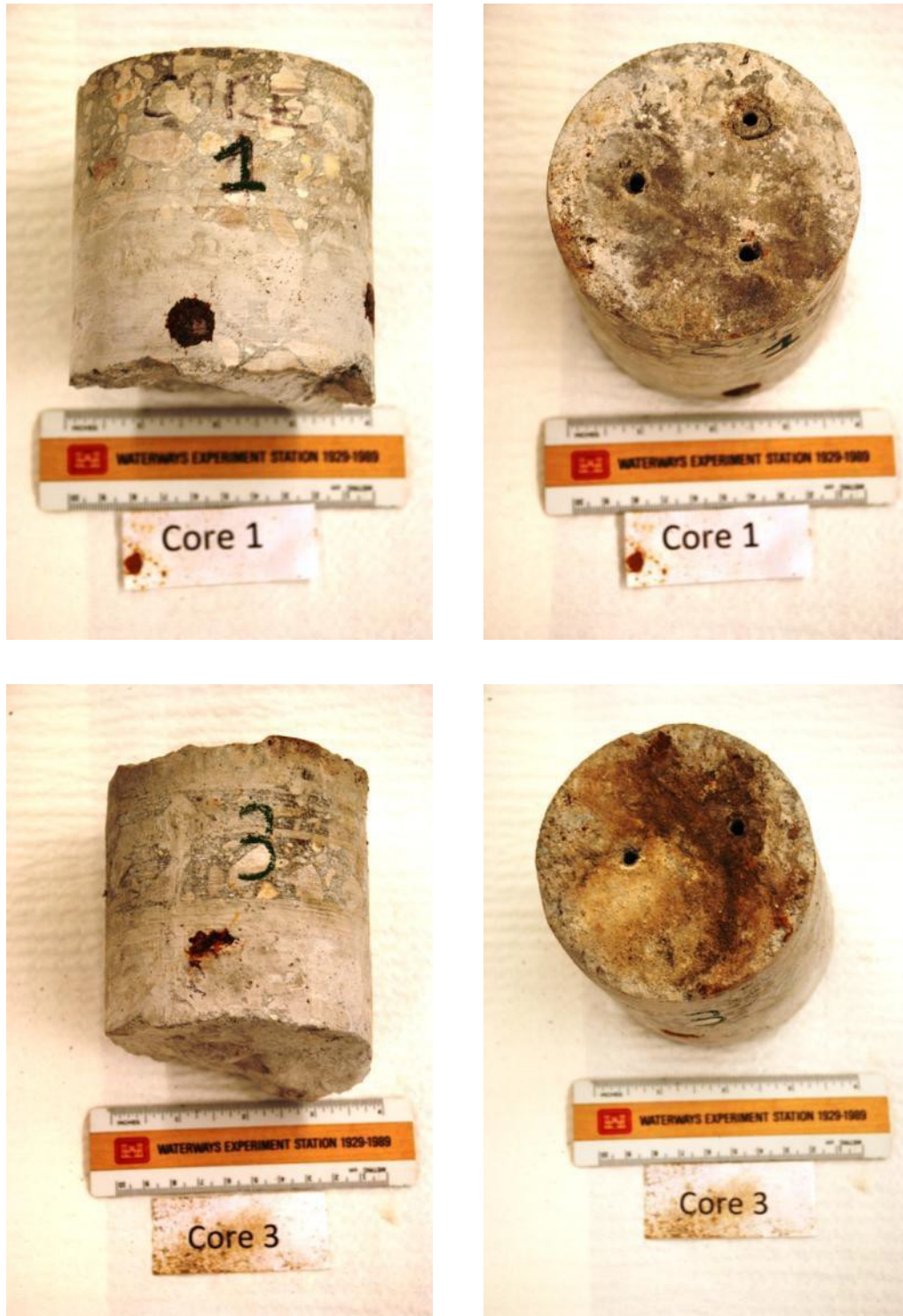


Figure C-1. Photos of as-received core samples #1 and #3.

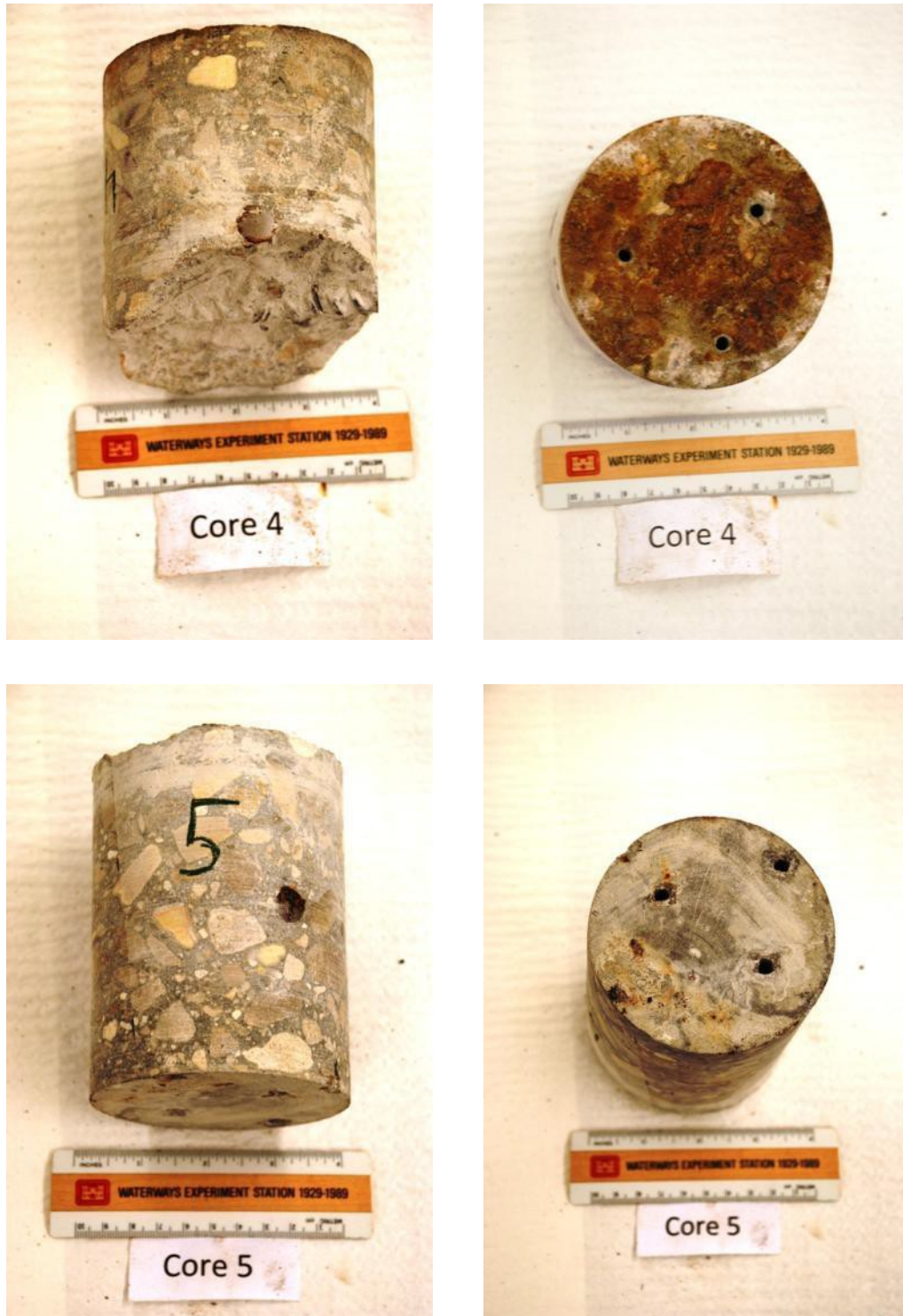


Figure C-2. Photos of as-received core samples #4 and #5.



Figure C-3. Photos of as-received core samples #6 and #7.



Figure C-4. Photos of as-received core samples #8 and #9.



Figure C-5. Photos of as-received core samples #10 and #11.



Figure C-6. Photos of as-received core samples #12 and #13.



Figure C-7. Photos of as-received core samples #14 and #15.



Figure C-8. Photos of as-received core samples #16 and #17.

Appendix D: Supplemental Photomicrographs

Figures D-1 – D-17 represent supplemental photomicrographs of core samples #1 and #3–16, as taken during the petrographic analyses done at ERDC-GSL, as discussed in Chapter 4.

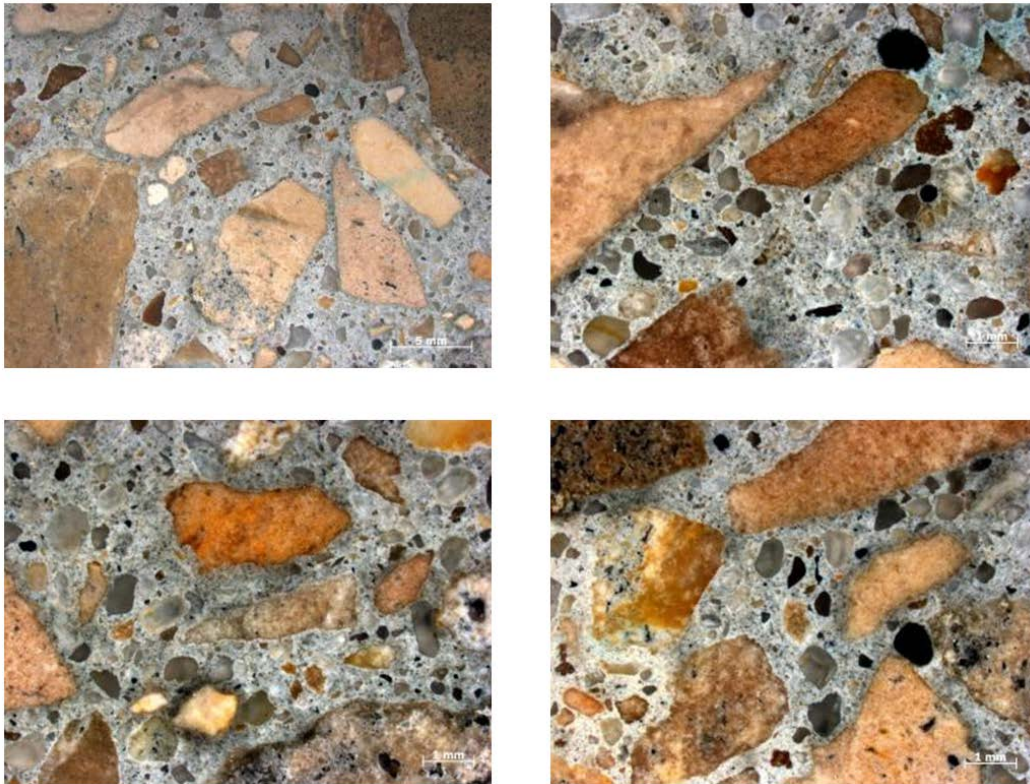


Figure D-1. Supplemental photomicrographs from core sample #1.

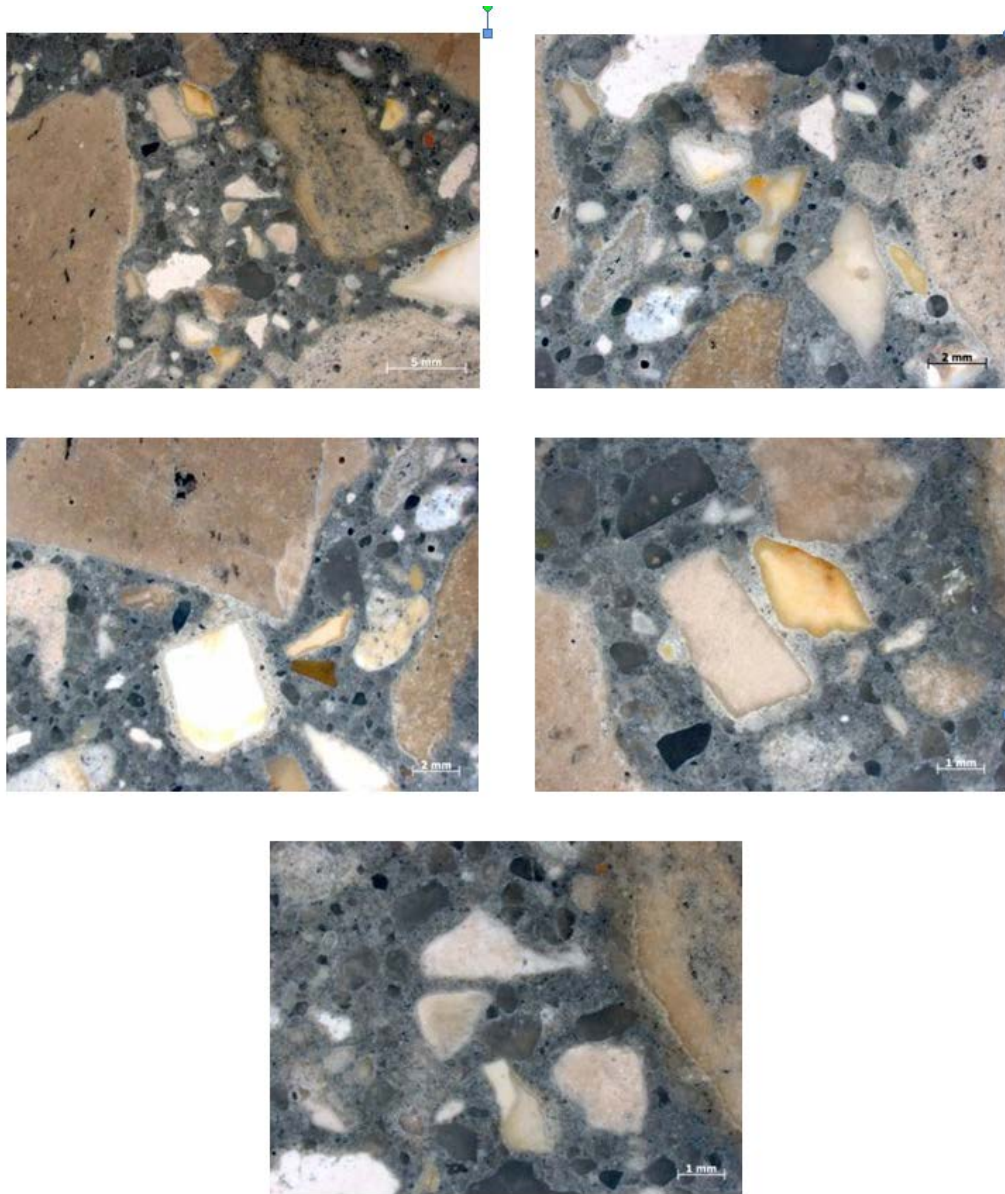


Figure D-2. Supplemental photomicrographs from core sample #3.

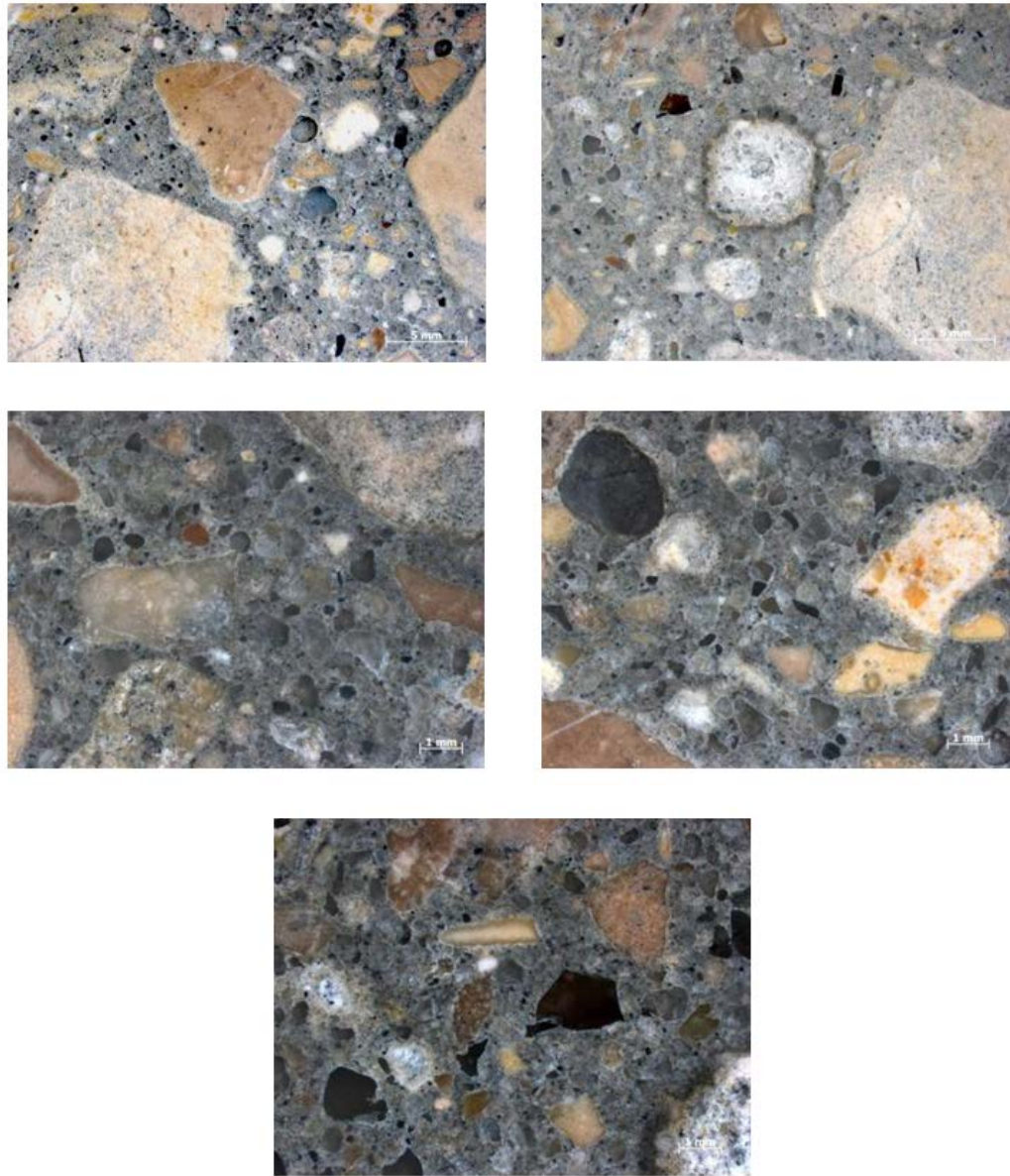


Figure D-3. Supplemental photomicrographs from core sample #4.

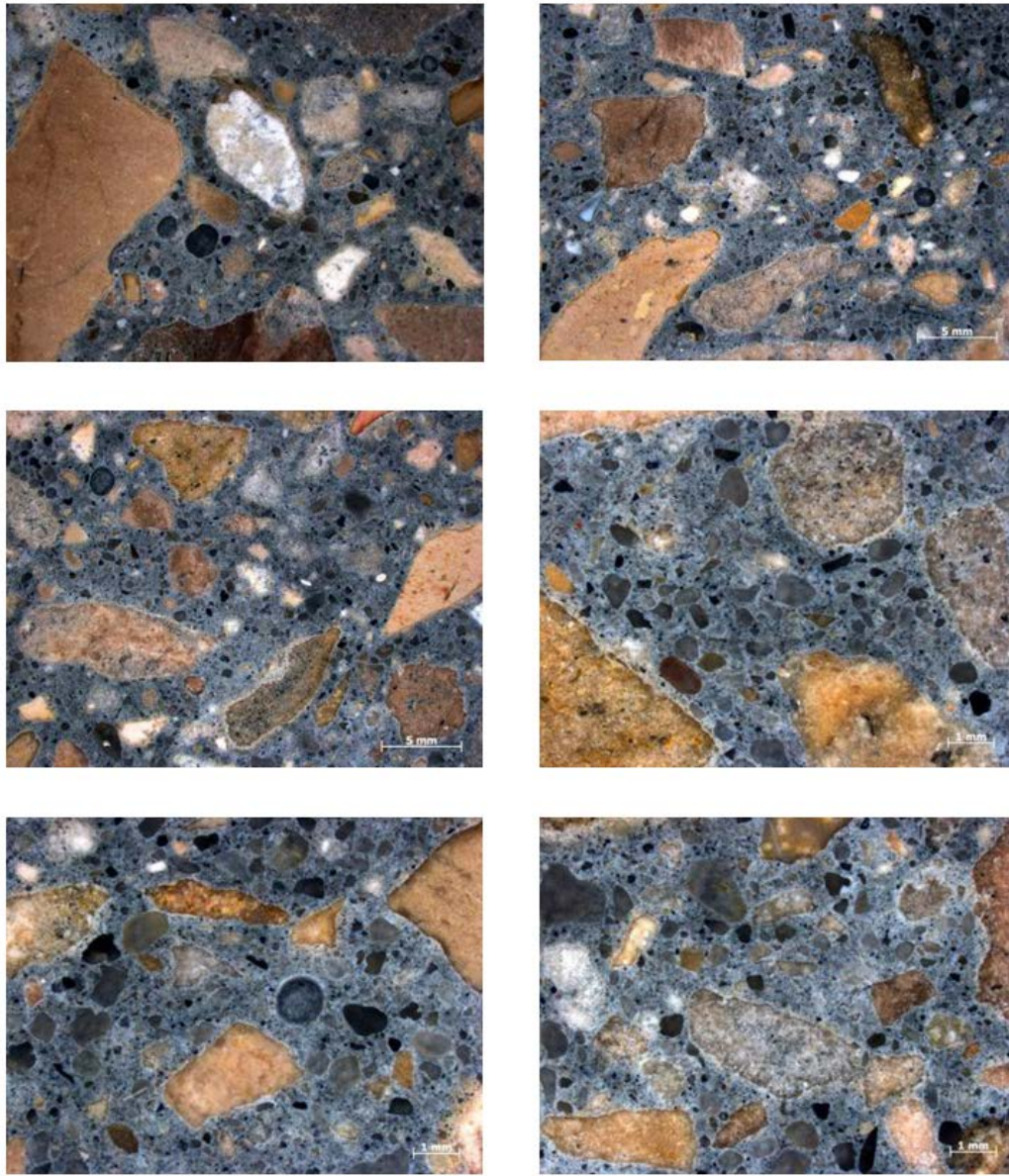


Figure D-4. Supplemental photomicrographs from core sample #5.

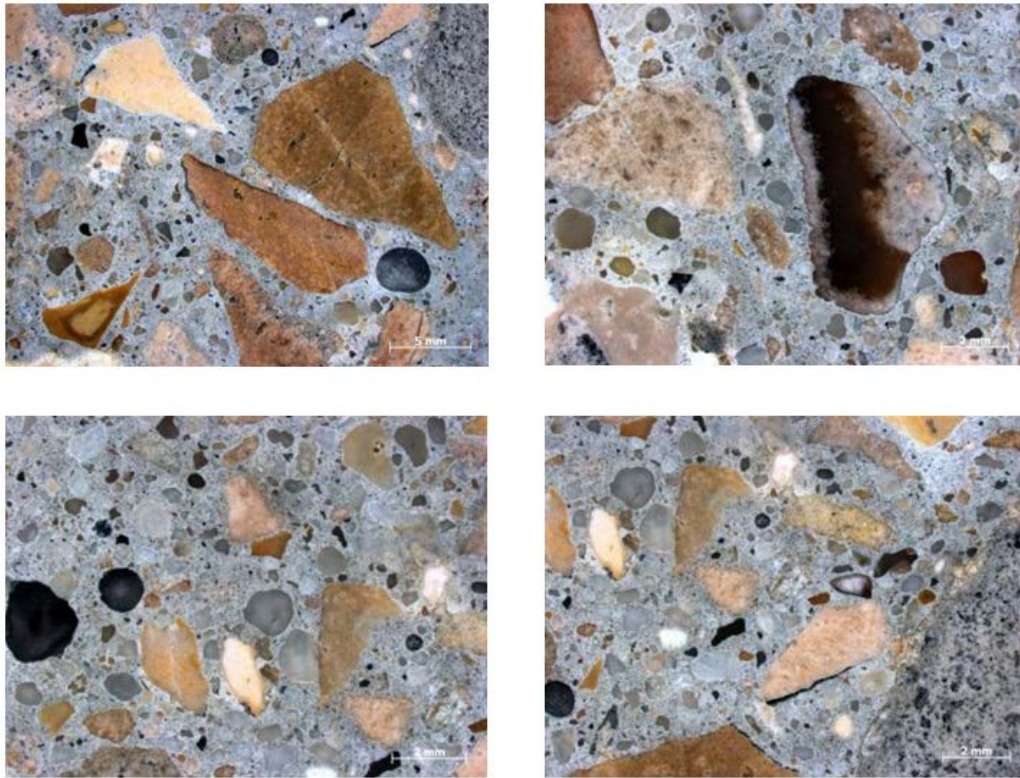


Figure D-5. Supplemental photomicrographs from core sample #6.

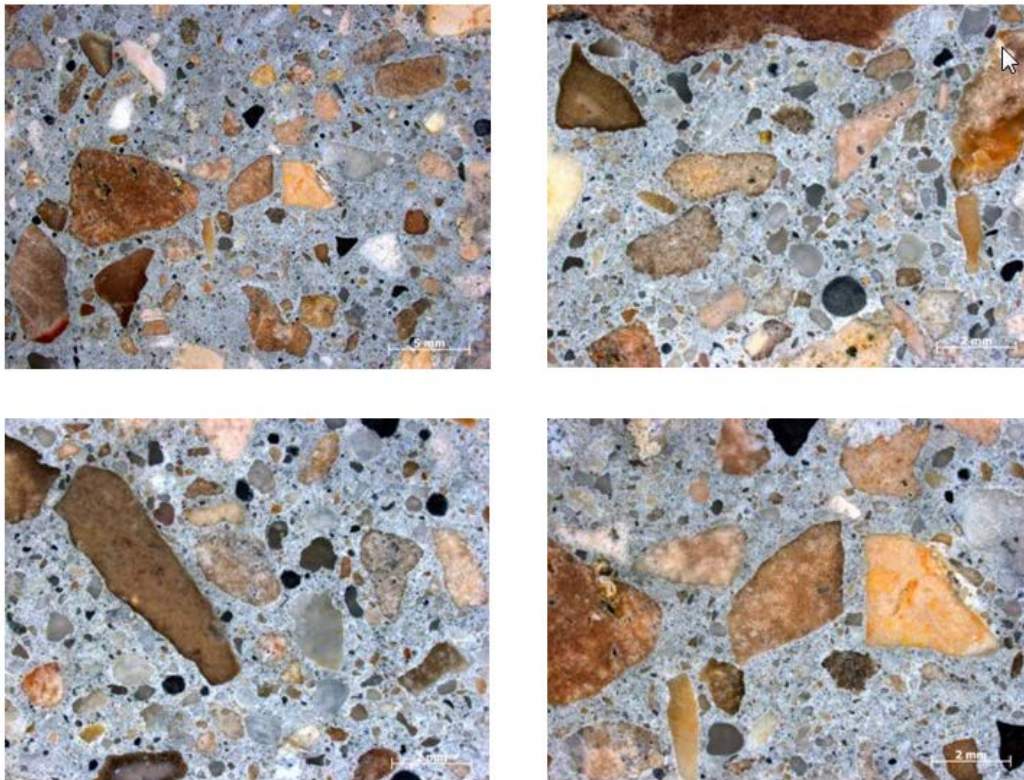


Figure D-6. Supplemental photomicrographs from core sample #7.

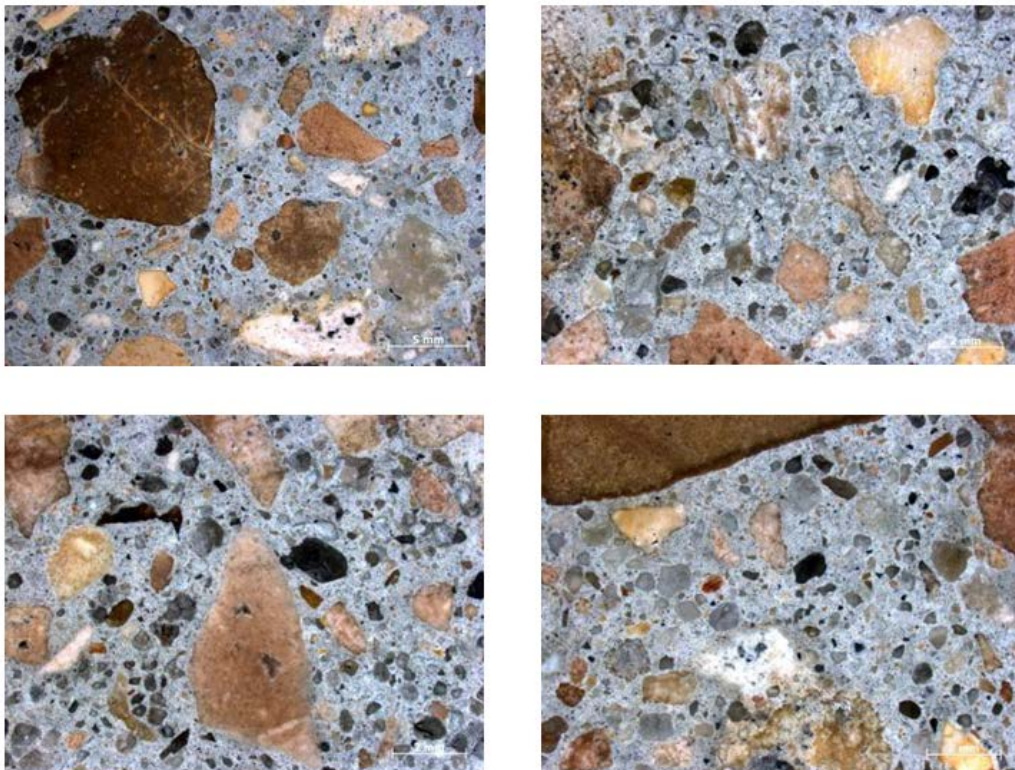


Figure D-7. Supplemental photomicrographs from core sample #8.

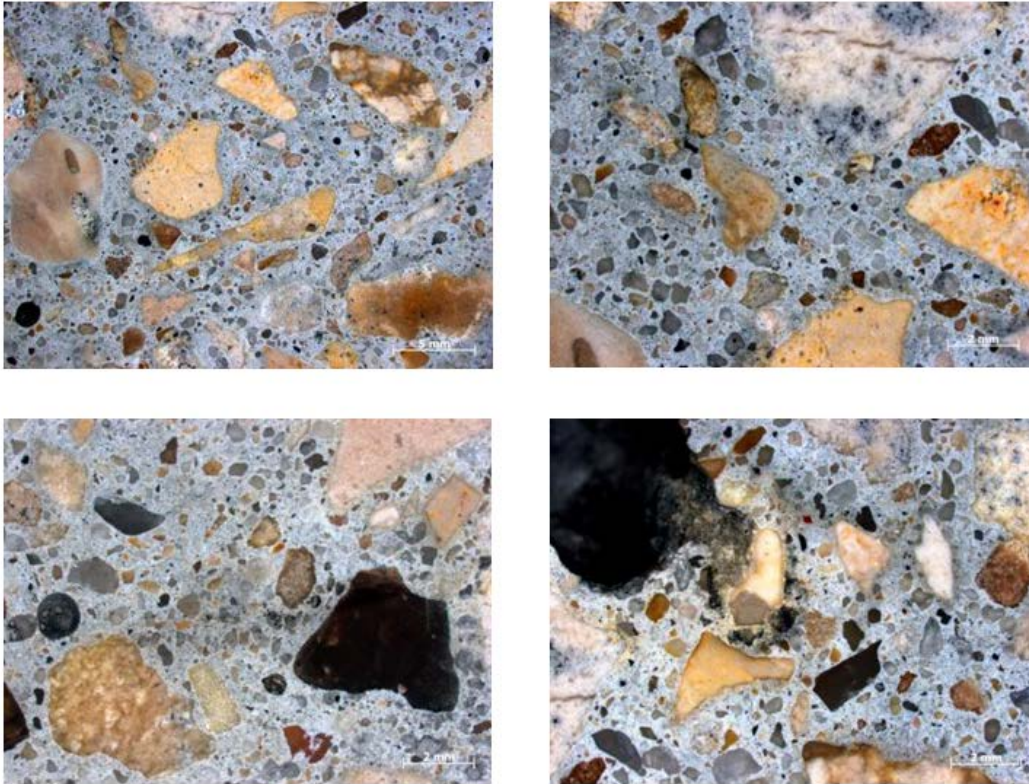


Figure D-8. Supplemental photomicrographs from core sample #9.

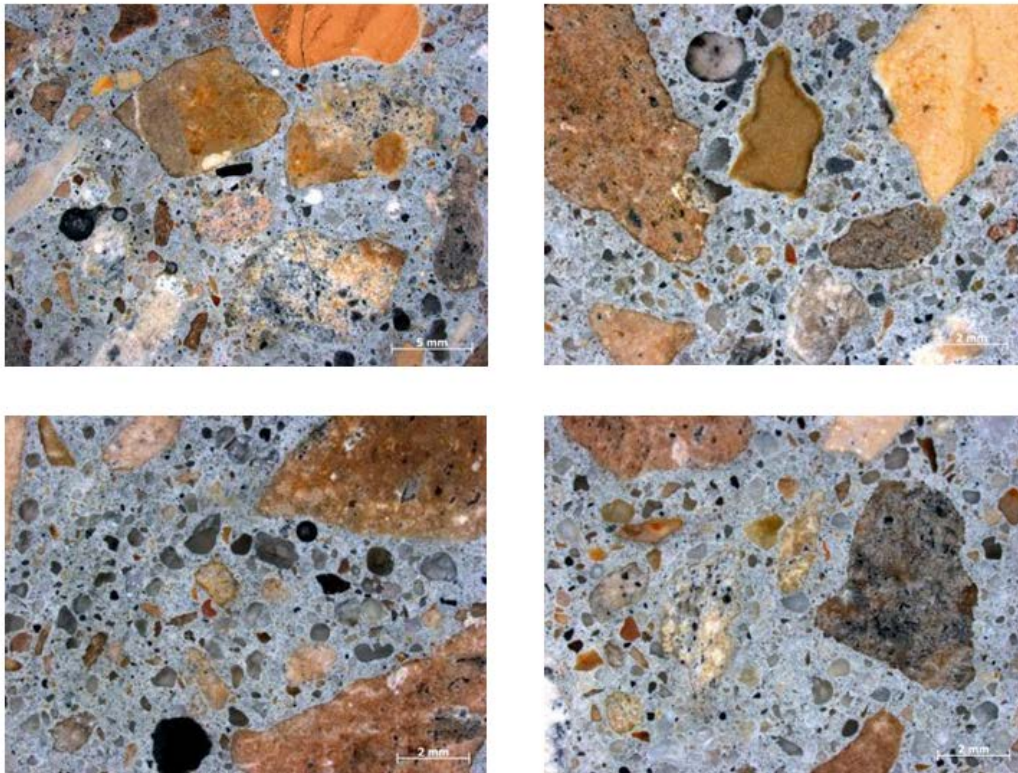


Figure D-9. Supplemental photomicrographs from core sample #10.

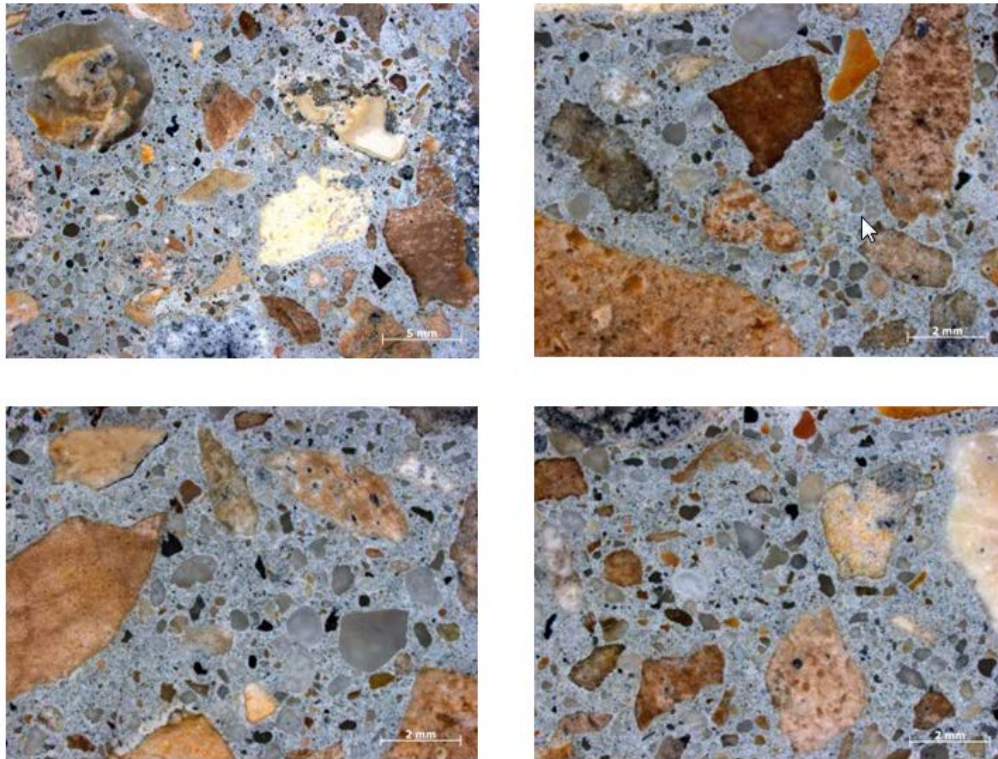


Figure D-10. Supplemental photomicrographs from core sample #11.

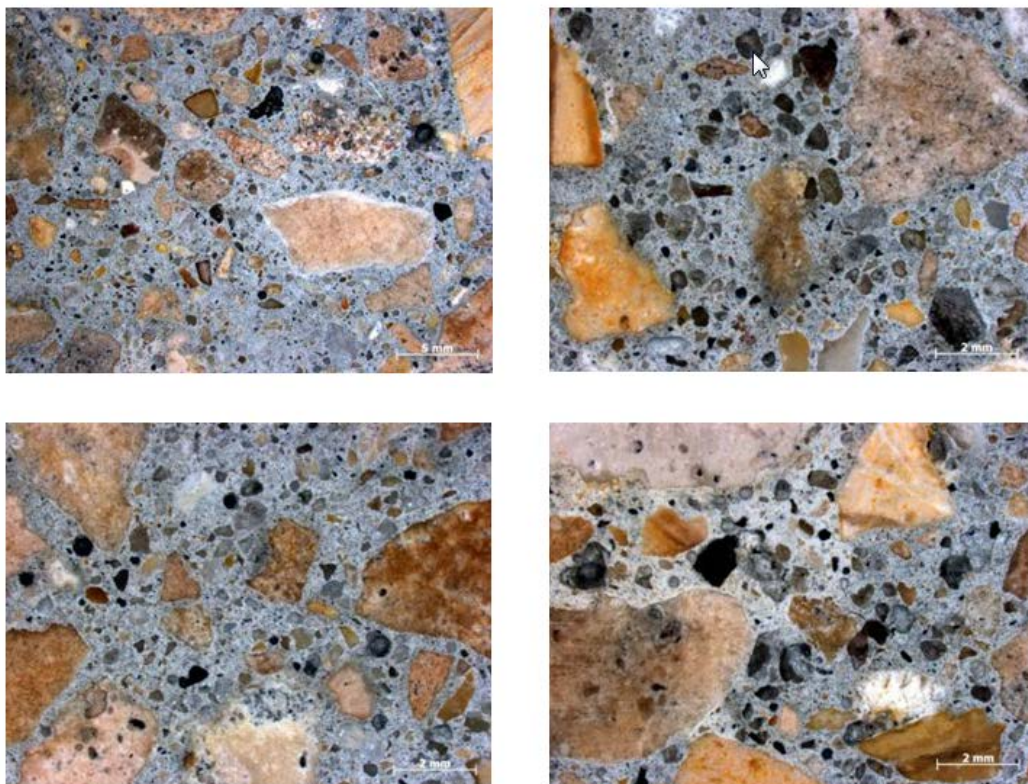


Figure D-11. Supplemental photomicrographs from core sample #12.

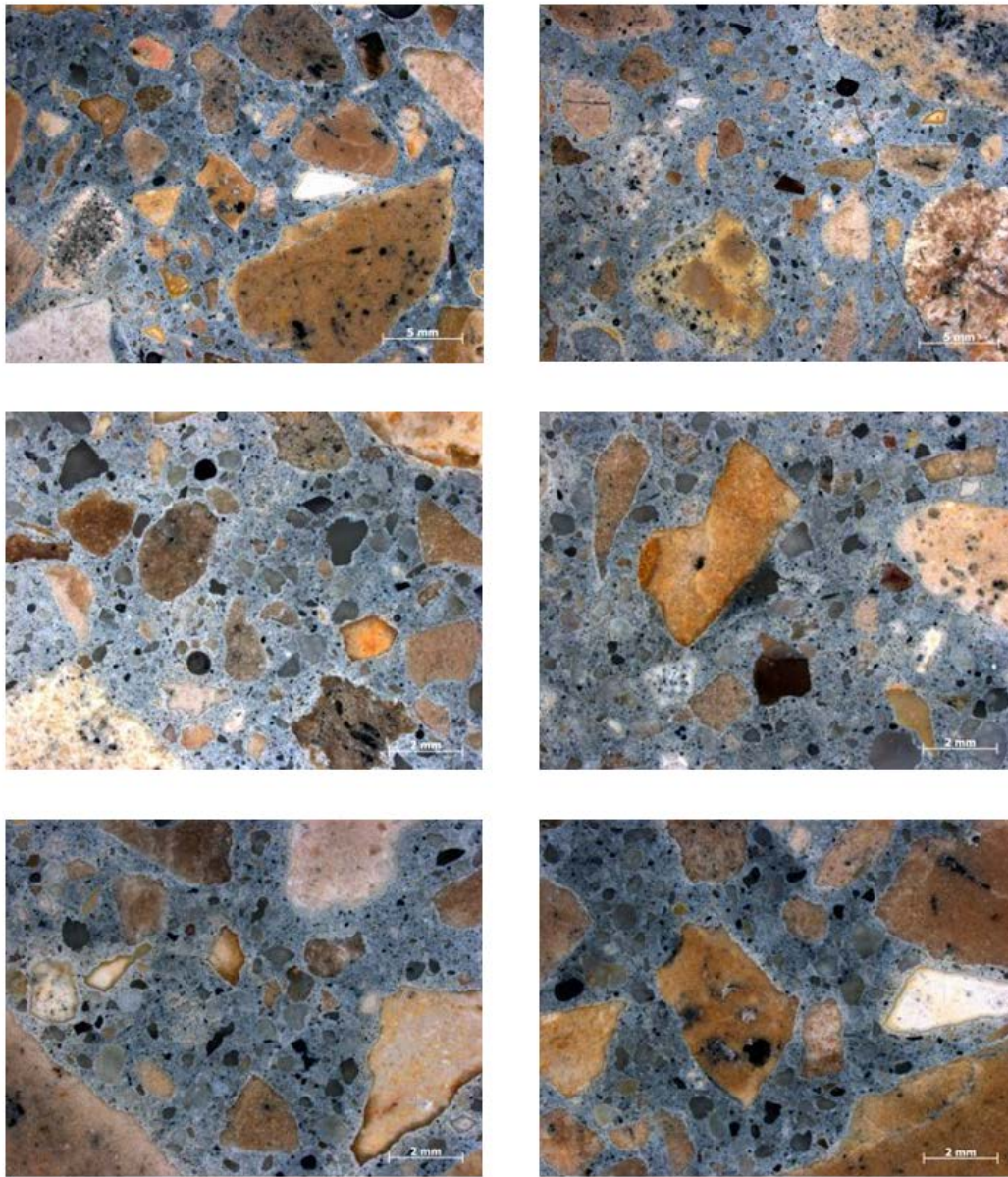


Figure D-12. Supplemental photomicrographs from core sample #13.

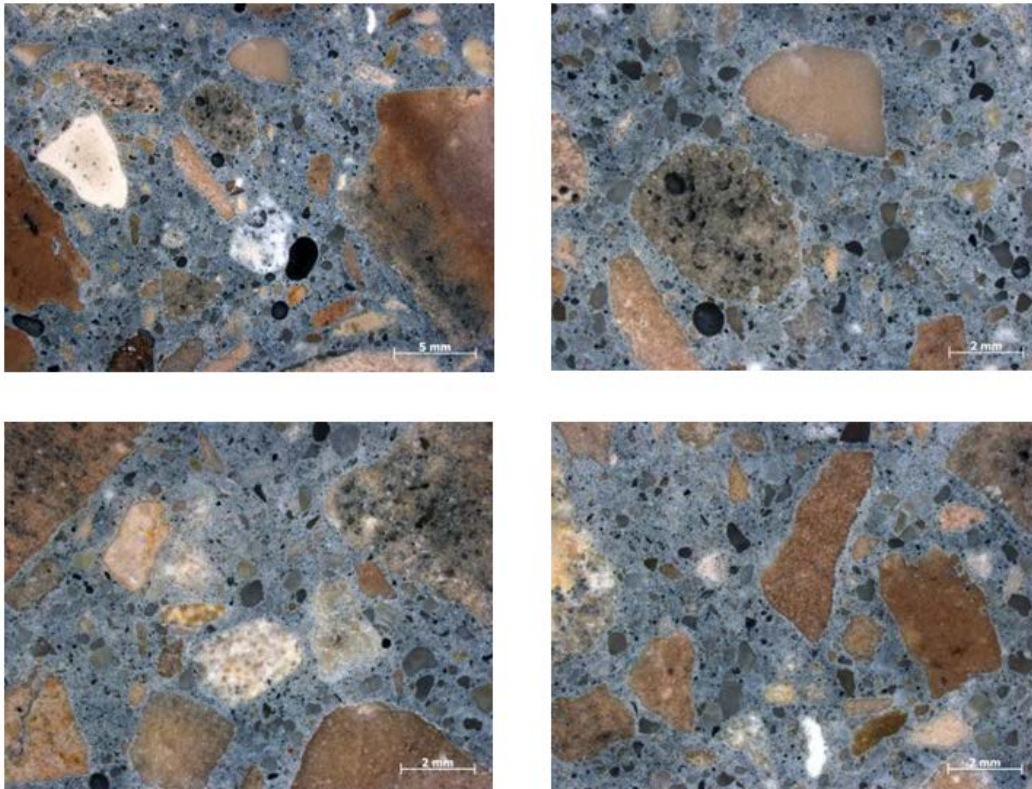


Figure D-13. Supplemental photomicrographs from core sample #14.

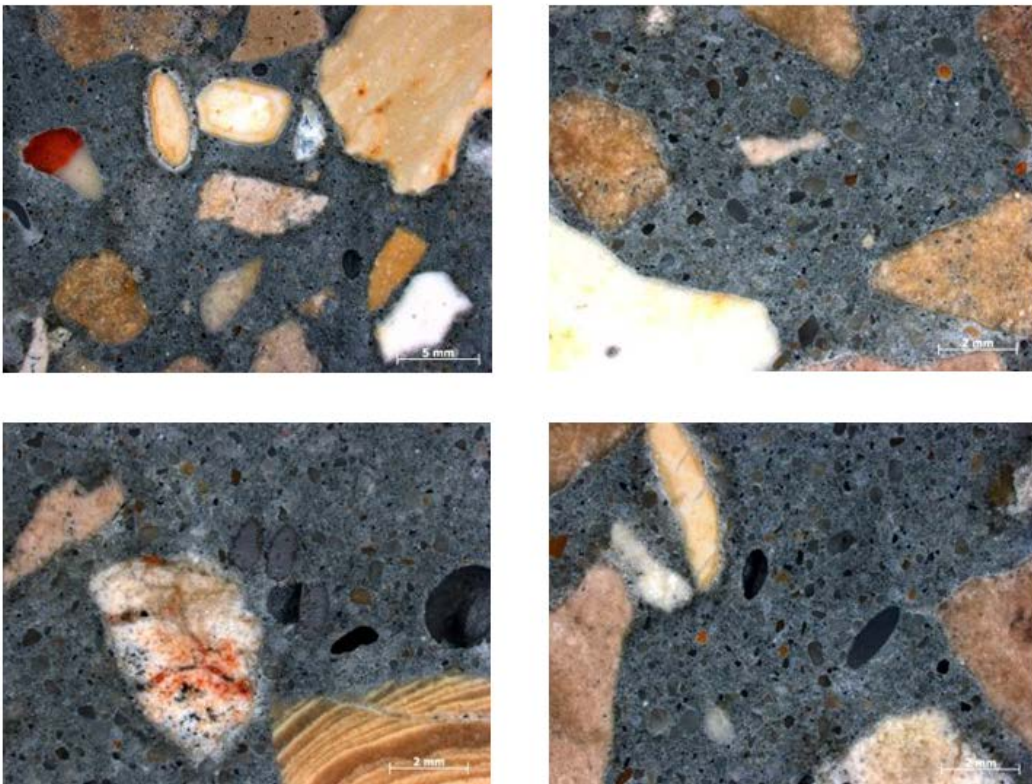


Figure D-14. Supplemental photomicrographs from core sample #15.

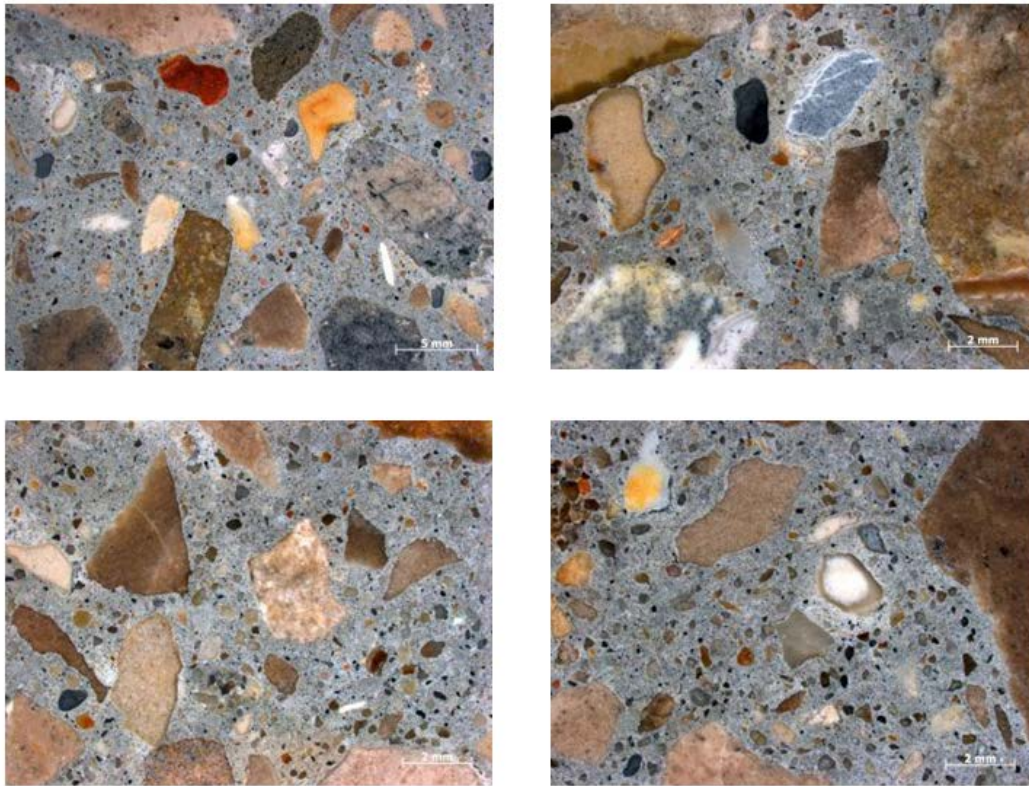


Figure D-15. Supplemental photomicrographs from core sample #16.



Figure D-16. Supplemental photomicrographs from core sample #17.

REPORT DOCUMENTATION PAGE

Form Approved
OMB No. 0704-0188

Public reporting burden for this collection of information is estimated to average 1 hour per response, including the time for reviewing instructions, searching existing data sources, gathering and maintaining the data needed, and completing and reviewing this collection of information. Send comments regarding this burden estimate or any other aspect of this collection of information, including suggestions for reducing this burden to Department of Defense, Washington Headquarters Services, Directorate for Information Operations and Reports (0704-0188), 1215 Jefferson Davis Highway, Suite 1204, Arlington, VA 22202-4302. Respondents should be aware that notwithstanding any other provision of law, no person shall be subject to any penalty for failing to comply with a collection of information if it does not display a currently valid OMB control number. PLEASE DO NOT RETURN YOUR FORM TO THE ABOVE ADDRESS.

1. REPORT DATE (DD-MM-YYYY) February 2013		2. REPORT TYPE Final		3. DATES COVERED (From - To)	
4. TITLE AND SUBTITLE Investigation of the Corrosion Mechanism and Determination of the EMS Estimated Service Life at Site 81				5a. CONTRACT NUMBER	
				5b. GRANT NUMBER	
				5c. PROGRAM ELEMENT NUMBER	
6. AUTHOR(S) Vincent F. Hock Jr., Charles A. Weiss Jr., Robert D. Moser, Sean W. Morefield, and James B. Bushman				5d. PROJECT NUMBER	
				5e. TASK NUMBER MIPR W2SD0622151436	
				5f. WORK UNIT NUMBER	
7. PERFORMING ORGANIZATION NAME(S) AND ADDRESS(ES) U.S. Army Engineer Research and Development Center (ERDC) Construction Engineering Research Laboratory (CERL) PO Box 9005 Champaign, IL 61826-9005				8. PERFORMING ORGANIZATION REPORT NUMBER ERDC SR-13-1	
9. SPONSORING / MONITORING AGENCY NAME(S) AND ADDRESS(ES) US Army Corps of Engineers Europe District CMR 410, Box 1, APO, AE 09049				10. SPONSOR/MONITOR'S ACRONYM(S) USACE-NAU	
				11. SPONSOR/MONITOR'S REPORT NUMBER(S)	
12. DISTRIBUTION / AVAILABILITY STATEMENT Approved for public release. Distribution is unlimited.					
13. SUPPLEMENTARY NOTES					
14. ABSTRACT <p>Structural damage resulting from corrosion of steel-clad structures can be of concern, especially when the steel is part of electromagnetic shielding of an underground structure. The US Army Corps of Engineers was called to lend assistance by having its corrosion experts and research laboratories investigate the condition and extent of corrosion at such a structure (Site 81) in Israel. This report documents the investigation, conclusions, and recommendations. In summary, from investigation and analyses of core samples, no significant corrosion was discovered and the estimated minimum service life of the existing structure is 199 years.</p>					
15. SUBJECT TERMS corrosion, steel, steel-clad structure, estimated minimum service (EMS), electromagnetic shielding (EMS)					
16. SECURITY CLASSIFICATION OF:			17. LIMITATION OF ABSTRACT UU	18. NUMBER OF PAGES 75	19a. NAME OF RESPONSIBLE PERSON
a. REPORT Unclassified	b. ABSTRACT Unclassified	c. THIS PAGE Unclassified			19b. TELEPHONE NUMBER (include area code)

Standard Form 298 (Rev. 8-98)

Prescribed by ANSI Std. Z39.18